HEI Research Report 240

Predictive, Source-Oriented Modeling and Measurements to Evaluate Community Exposures to Air Pollutants and Noise from Unconventional Oil and Gas Development

Lea Hildebrandt Ruiz et al.

Additional Materials C: Chapter 5

Correspondence may be addressed to Dr. Lea Hildebrandt Ruiz, The University of Texas at Austin, 200 E. Dean Keeton St., Austin, TX 78712; email: lhr@che.utexas.edu.

Although this report was produced with partial funding by the United States Environmental Protection Agency under Contract No. 68HERC19D0010 to the Health Effects Institute, it has not been subjected to the Agency's peer and administrative review and may not reflect the views of the Agency; thus, no official endorsement by the Agency should be inferred. This report also has not been reviewed by private party institutions, including those that support HEI Energy, and may not reflect the views or policies of these parties; thus, no endorsement by them should be inferred.

atmosphere

Additional Materials C: Chapter 5

MDPI

Article

Spatial and Temporal Variability in Atmospheric Emissions from Oil and Gas Sector Sources in the Marcellus Production Region

Qining Chen, Nadin Raksi, Lily Niewenhous, Sewar Jennifer Almasalha, Joel D. Graves, V'Jae Brown, Shannon Stokes, David T. Allen * and Lea Hildebrandt Ruiz

Center for Energy and Environmental Systems Analysis, The University of Texas at Austin, Austin, TX 78759, USA; qnchen@utexas.edu (Q.C.); nadinraksi@utexas.edu (N.R.); lgn346@my.utexas.edu (L.N.); sewar@utexas.edu (S.J.A.); joel.graves@austin.utexas.edu (J.D.G.); vjae.brown@utexas.edu (V.B.); stokessn@austin.utexas.edu (S.S.); lhr@che.utexas.edu (L.H.R.)
* Correspondence: allen@che.utexas.edu

Abstract

Temporal variability in emissions from oil and gas supply chains depends on the spatial scale at which emissions are aggregated. This work demonstrates a framework for simulating temporally and spatially resolved emission inventories that can be broadly applied in oil and gas production regions. Emissions of methane, ethane, volatile organic compounds (VOCs), and nitrogen oxides (NOxs) from oil and gas facilities in the Marcellus production region were estimated at a one-hour time resolution for the calendar year 2023 and were aggregated at the grid cell (4 km by 4 km), county, and basin level. Maximum to average emission rate ratios decreased as the scale of spatial aggregation increased and differed by pollutant. At the grid cell level, ratios of maximum to average emission rates exceeded 100 in some grid cells for VOCs. In contrast, basin level maximum to average ratios for NOx emission rates were less than 1.1. The sources driving temporal variability in hydrocarbon emissions were well completions and liquid unloadings, while the sources driving temporal variability in NOx emissions were preproduction activities such as drilling and hydraulic fracturing. Temporally and spatially resolved inventories can inform pollutant- and region-specific measurement campaigns and mitigation strategies. Reconciliation between inventories and observations must consider event frequency, duration, and persistence, along with the spatial scale and timing of measurements.

Keywords: emission variability; spatial variability; temporal variability; methane emissions; ethane emissions; volatile organic compounds (VOCs); nitrogen oxides (NOxs); oil and gas production; spatial aggregation; Marcellus

Academic Editor: Wei-Ping Hu

Received: 15 July 2025
Revised: 16 August 2025
Accepted: 28 August 2025
Published: 3 September 2025

Citation: Chen, Q.; Raksi, N.; Niewenhous, L.; Almasalha, S.J.; Graves, J.D.; Brown, V.; Stokes, S.; Allen, D.T.; Hildebrandt Ruiz, L. Spatial and Temporal Variability in Atmospheric Emissions from Oil and Gas Sector Sources in the Marcellus Production Region. *Atmosphere* **2025**, *16*, 1048. https://doi.org/10.3390/atmos16091048

1. Introduction

Emissions of greenhouse gases and criteria air pollutants from oil and gas supply chains have complex spatial and temporal patterns [1]. For example, emission rates for methane from individual sources can vary over six orders of magnitude, from grams per hour to tons per hour [2], but the highest emission rate sources generally have short durations, while lower emission rate sources can be both long and short duration [3]. If ensembles of instantaneous measurements are made at oil and gas production sites, methane emissions follow a highly skewed distribution, with the sites with the highest instantaneous emission rates (top 5%) contributing >50% of total emissions [4]. The overall magnitude of emissions and their spatial and temporal patterns can vary by basin. Collectively, and

integrated over time, production-normalized methane emissions at the basin level ranged from <1% to 5% among major oil and gas basins in the United States [4,5]. Emissions of volatile organic compounds (VOCs) also have temporal and spatial variability [6], but the sources of that variability are different than the sources of variability in methane and other light alkane emissions [7]. Emissions of nitrogen oxides (NOxs) also exhibit variability [8], but again, the sources are different than the sources that drive variability in methane and VOCs emissions [9].

The magnitude of temporal variability in emissions depends not only on the pollutant but also on the spatial scale at which emissions are aggregated. The smaller the spatial scale of aggregation, the larger the temporal variability. Discrete measurement campaigns at the same well site showed significant variability in methane emissions, with emission rates varying by nearly 50-fold across six measurement campaigns over a 21-month period [10] and by more than 550 times across 17 campaigns conducted over four years [11]. Even greater variability will be observed if emissions are monitored continuously [12,13]. Temporal variability in emissions from individual sites will generally be greater than variability in emissions aggregated over a grid cell containing dozens of sites; grid cell variability will be greater than the variability at the county level, which will be greater than the variability at the basin level. No prior research has systematically examined how temporal variability in emissions vary, as emissions are aggregated across various spatial scales.

There are multiple human health implications associated with spatial and temporal variability in emissions. Examples of potential impacts include, but are not limited to, variability in ozone productivity driven by local variability in emissions of NOx, particularly when coupled with high emissions of biogenic hydrocarbons and localized exposures to elevated levels of criteria or hazardous air pollutants [9]. Spatial and temporal variability in emissions is also important to consider when using short duration measurements, such as aircraft overflights, in estimating longer term emissions. The magnitude, frequency, and duration of episodic emissions will determine how many measurements will be needed to accurately predict long-term emissions [14–16].

This work will demonstrate methods for modeling spatial and temporal variability in emissions from oil and gas sources by estimating the routine emissions associated with the production and midstream processing of oil and gas produced by more than 200,000 sites in the Marcellus production region in the United States. Year-long time series of emissions will be estimated at one-hour resolution for methane, ethane, VOCs, and NOx. Emissions will be aggregated at the grid cell (4 km by 4 km), county, and basin level, and at each of these spatial scales, distributions of expected emission rates will be characterized.

The framework and simulation methods developed in this work can be broadly applied in other oil and gas production regions to characterize both spatial and temporal variability in hydrocarbon and NOx emissions. Understanding these pollutant-specific temporal and spatial characteristics is essential for developing pollutant-specific measurement campaigns and mitigation strategies. Current national and regional emission inventories, such as the U.S. Greenhouse Gas Inventory (GHGI) [17], the National Emissions Inventory (NEI) [18], the Greenhouse Gas Reporting Program (GHGRP) [19], and emission inventories developed by state governments for air quality management [20], typically report annual average emissions and do not capture temporal variability in emissions from oil and gas sources. This work provides a pathway to develop spatially and temporally resolved emission inventories based on publicly available information and enables a more accurate representation of emissions. Inventories for the Marcellus oil and gas production region in the northeastern United States are developed to demonstrate the methods.

2. Materials and Methods

2.1. Study Domain

Figure 1 shows the study domain and locations of simulated sources. The study domain was divided into 4 km by 4 km grid cells covering 98% of active production wells reported in the Marcellus Shale [21]. A total of 201,338 wells, drilled on or before 2023 and actively producing in 2023, are included in the simulation, representing production and emission scenarios in the year 2023. The gridded area includes grid cells without any reported production, and these grid cells will be assumed to have no emissions associated with upstream and midstream oil and gas operations.

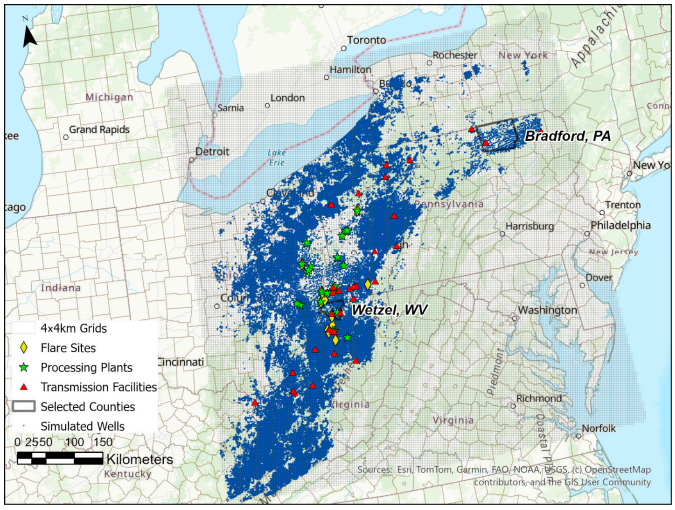

Figure 1. Well sites, midstream sites, and flares included in the simulation within the study domain overlapped by 4 km-by-4 km grid cells.

Emission sources in the study domain include well-level emissions from preproduction and production activities on active well sites, emissions from midstream operations, and emissions from flaring. Active well sites were identified based on production data [21]. Well site emissions in two counties, Bradford, PA, USA and Wetzel, WV, USA were used as representative regions to compare county-level emissions to emissions resolved at the grid cell level. Bradford County is located in the northeast portion of the basin, a relatively dry gas production region with mostly unconventional horizontally drilled wells. Wetzel County is in the southwest portion of the basin and has a large amount of liquids production compared to Wetzel County, from comparable numbers of conventional and unconventional wells. Distributions of well types included in the study domain and in two selected counties are shown in Table 1. Aggregated production data in the study domain and in the two selected counties are available in Supporting Information (SI).

Table 1. Well types in the study domain and two selected counties.

Location	Wells in Simulation							Wells Eliminated
	Total	Horizontal/ Directional	Vertical	Dry Gas [1]	Wet Gas [2]	Oil [3]	Wells Completed in 2023	No Production or Missing Production Data in 2023 or Completed After 2024
Study domain	201,338	20,902	174,536	123,170	42,305	35,863	1438	11,449
Bradford, PA, USA	1520	1507	13	1520	0	0	75	199
Wetzel, WV, USA	1295	541	754	606	491	198	50	177

[1] Dry gas wells are wells with <1% liquids production in wellhead stream. [2] Wet gas wells include wells classified as wet gas wells (1–10% liquids in wellhead stream) and liquid-rich gas wells (10–40% liquids in wellhead stream). [3] Oil wells are wells with >40% liquids production in wellhead stream.

Midstream sites include gathering and boosting stations (assumed one per grid cell), gas processing plants, and transmission facilities. Gas processing plants and transmission facilities were drawn from the EPA Greenhouse Gas Reporting Program (GHGRP) [19] and manually verified based on satellite images [22]. Flare locations were based on annual gas flare estimates with Visible Infrared Imaging Radiometer Suite (VIIRS) observations in 2023 [23]. Only midstream flares and flares located in grid cells with active wells were included in the simulation.

2.2. Spatial Aggregation

Emissions were aggregated and are reported at three spatial levels: the grid cell level, the county level, and the basin level. These levels of reporting involved 2 types of aggregation: pre-simulation and post-simulation. Pre-simulation refers to the aggregation of activity data (e.g., production volumes and equipment counts) prior to emission simulation. Post-simulation refers to the aggregation of simulated emissions. Post-simulation aggregation at individual well sites and midstream sites was carried out in Bradford and Wetzel Counties. These simulations will be used to compare grid-cell-level aggregation of emissions to county-level aggregation of emissions. To compare county-level aggregation of emissions to basin-level aggregation of emissions, sources were aggregated pre-simulation at the county level.

For wells in Bradford and Wetzel Counties, well site emissions were simulated based on estimated equipment and operation counts at individual well sites. Emissions from gathering, processing, and transmission sites and flares were simulated as total site-level emissions. These emissions were spatially aggregated by grid cell and by county over the 2023 year-long time series. Bradford County includes a total of 1520 wells, with 1216 wells located within 132 grid cells that are completely within the county boundary. Wetzel County includes 1295 wells, with 840 wells distributed across 36 grid cells that are fully within the county. Only wells within grid cells that are completely within county boundaries were included in spatial aggregation.

For county-level and basin-level reporting based on county-level simulations, well sites were aggregated pre-simulation. Up to three "aggregated wells" were created for each county: one dry gas well representing all dry gas wells, one wet gas well representing all wet gas wells, and one oil well representing all oil wells within the county. Production volumes and equipment counts were summed and assigned to their corresponding aggregated well. Detailed aggregation and simulation methods, by source, are described in the following sections.

2.3. Emission Compositions

Emission compositions at the well level were simulated using the Emission Composition Tool, built into the Methane Emission Estimation Tool (MEET V1.1) [24]. The Emission Composition Tool is a searchable database constructed with field measurement data and thermodynamic models and can be queried to estimate hydrocarbon compositions from various emission sources at oil and gas production sites by matching input parameters, including gas-to-oil ratios, API gravity, separator temperature and pressure, and produced gas compositions [25]. Three emission composition profiles were generated in this work: dry, wet, and oil. Input parameters for "dry" and "wet" profiles were estimated based on the averaged parameters from dry gas and wet gas wells measured in the Marcellus production region [26]. Input parameters for the "oil" profile were from multiple sources. Gas-to-oil ratio was calculated based on production data in the basin in 2023 [21]. API gravity, separator pressure, and produced gas compositions were the averaged values across a subset of wells from the Central Appalachian Basin Natural Gas Database [27].

The subset included wells with an API gravity lower than 45 and non-zero produced gas compositions. While the database did not provide information on separator temperature, separator temperature for the "oil" profile was assumed to be the same as that for the "wet" profile. Input parameters for estimating each composition profile are summarized in Table 2.

Table 2. Input parameters for estimating emission compositions using the Emission Composition Tool.

	Well Production		Separator		Produced Gas Compositions		
Profile ID	**Gas-to-Oil Ratio (SCF/BBL)**	**API Gravity**	**Separator Temperature (°F)**	**Separator Pressure (Psia)**	**Methane (Molar Fraction)**	**Ethane (Molar Fraction)**	**Propane (Molar Fraction)**
Dry	NA	NA	63.1	278	97.4%	2.11%	0.0753%
Wet	427,083	65.7	72	97.5	76.8%	14.9%	4.95%
Oil	5206	14.4	72	898	51.9%	13.7%	7.77%

Table 3 shows estimated emission compositions returned by the Emission Composition Tool [25], based on input parameters in Table 2. Four sets of emission compositions were estimated for each composition profile, including wellstream, produced gas, water tank flash, and condensate tank flash. While the tool did not simulate VOC emissions from condensate tank flash, the sum of propane and butane emissions was used as a surrogate for VOCs and is reported in Table 3. Emission compositions from the dry composition profile were assigned to emissions from dry gas wells; wet profile compositions were assigned to wet gas wells, and oil profile compositions were assigned to oil wells. There were a few wells characterized as dry gas wells in the production database [21] but with non-zero oil production. Since the dry profile assumed no oil production, wet profile compositions were re-assigned to these wells.

Table 3. Estimated emission compositions applied in inventory development.

Composition profile: dry					
Compositions	Methane	Ethane	Propane	Butanes [1]	VOCs
Wellstream (molar fraction)	97.9%	1.14%	0.0174%	0.0004%	0.0178% (44.3 g/mol)
Produced gas (molar fraction)	97.9%	1.14%	0.0174%	0.0004%	0.0178% (44.3 g/mol)
Water tank flash (kg/bbl)	0.0824	2.75×10^{-3}	5.10×10^{-5}	1.30×10^{-6}	5.23×10^{-5}
Condensate tank flash (kg/bbl)	NA	NA	NA	NA	NA
Composition profile: wet					
Compositions	Methane	Ethane	Propane	Butanes [1]	VOCs
Wellstream (molar fraction)	40.6%	20.5%	16.9%	10.35%	37.9% (68.5 g/mol)
Produced gas (molar fraction)	63.4%	23.2%	9.55%	2.21%	12.1% (47.3 g/mol)
Water tank flash (kg/bbl)	0.0626	0.0794	0.0438	0.0350	0.0893
Condensate tank flash (kg/bbl)	3.51	16.5	40.8	43.6	84.4 [2]
Composition profile: oil					
Compositions	Methane	Ethane	Propane	Butanes [1]	VOCs
Wellstream (molar fraction)	40.6%	20.5%	16.9%	10.4%	37.9% (68.5 g/mol)
Produced gas (molar fraction)	50.4%	24.2%	16.7%	6.43%	24.3% (49.2 g/mol)
Water tank flash (kg/bbl)	0.0149	0.0248	0.0229	0.0289	0.0648
Condensate tank flash (kg/bbl)	0.381	2.67	12.0	23.4	35.4 [2]

[1] Sum of n-butane and isobutane. [2] Calculated as the total mass of propane and butanes in condensate tank flash.

2.4. Emission Sources

Table 4 summarizes all emission sources and pollutants included in the simulation, the emission estimation method and hydrocarbon compositions for emission estimates, and whether the source was aggregated pre-simulation for county- and basin-level reporting. Hydrocarbon compositions were sourced from the EPA 2020 Nonpoint Oil and Gas Emission Estimation Tool (referred to as EPA Oil and Gas Tool in the following text) [28], and/or from the Emission Composition Tool [25]. The 2020 version of the EPA Oil and Gas Tool was used because it was the most recent version with complete documentation at the time the simulations were performed. The composition of throughput gas for midstream facilities and the composition of flared gas at the grid cell level was estimated by combining production and produced gas compositions from individual wells. Throughput gas compositions estimated at the level of counties were used to estimate emissions from combustion sources that included artificial lift engines and heaters, assuming local produced gas was used as fuel. The sources without pre-simulation aggregation were always simulated at the individual well level and aggregated during post-processing.

For some of the simulated sources, activity data used in equipment assignments were sourced from the 2022 Inventory of U.S. Greenhouse Gas Emissions and Sinks (GHGI) [29], shown in Table 5. The 2022 data was the most recent version available at the time the simulations were performed. The GHGI reports two sets of activity factors for the natural gas system and the petroleum system. Activity factors reported for the natural gas system were applied to dry gas wells, and activity factors reported for the petroleum system were applied to the oil wells. For wet gas wells, the activity data was assigned as the average data for dry gas and oil wells. If the equipment or operation category does not exist in the petroleum system, or is not applicable to oil wells, such as gas meters/piping and liquid unloading operations, the activity factors reported for the natural gas system were consistently applied to both dry and wet gas wells. The equipment assignments based on this activity data are described in the Supporting Information (SI).

Detailed simulation methods per emission source are available in the SI. Briefly, emissions per source were simulated by combining activity factors, emission factors, and composition data from various publicly available databases. Hydrocarbon emissions from most non-combustion sources at well sites were simulated using the Methane Emission Estimation Tool (MEET) V1.1 [24]. Hydrocarbon emissions from associated gas venting and hydrocarbon and NOx emissions from combustion sources at well sites were simulated using the EPA Oil and Gas Tool [28]. Hydrocarbon emissions from gathering and boosting sites were estimated based on throughput gas flowrates and compositions. Hydrocarbon emissions from gas procession and transmission sites were estimated based on the EPA Greenhouse Gas Reporting Program [19] and throughput gas compositions. NOx emissions from gathering and boosting, processing, and transmission sites were estimated based on methane emissions, fraction of combustion sources, and the EPA AP-42 emission factors for stationary internal combustion sources [30]. For flares, hydrocarbon emissions were estimated based on satellite detections, and NOx emissions were estimated based on methane emissions and EPA AP-42 emission factors for flaring [30].

The simulation methods for well site non-combustion sources were evaluated against observations by Graves et al. [31]. Simulated ethane inventories coupled with site-level dispersion modeling for thousands of sites were summed and compared with ethane measurements at a regional air quality monitor in the Eagle Ford oil and gas production region. Predictions of routine emissions, coupled with dispersion modeling, accurately captured diurnal profiles of observations up to the 95th percentile of observations. Simulated routine emissions accounted for one third of the highest (>99th percentile) daytime concentrations observed and two thirds of the highest nighttime concentrations observed.

Table 4. Emission sources and estimation method.

Emission Sites	Emission Sources	Simulated Pollutants	Main Method for Emission Estimates	Hydrocarbon Compositions	Pre-Aggregation
Well sites: preproduction	Drilling engines	Methane, VOCs, NOx	EPA Oil and Gas Tool [28]	EPA Oil and Gas Tool	Not aggregated
	Hydraulic fracturing pumps	Methane, VOCs, NOx	EPA Oil and Gas Tool [28]	EPA Oil and Gas Tool	Not aggregated
	Completion flowbacks	Methane, Ethane, VOCs	MEET [24]	Wellstream	Not aggregated
Well sites: production	Artificial lift engines	Methane, ethane, VOCs, NOx	EPA Oil and Gas Tool [28]	County-throughput-produced gas composition and EPA Oil and Gas Tool	Aggregated
	Associated gas venting	Methane, ethane, VOCs	EPA Oil and Gas Tool [28]	Produced gas	Aggregated
	Condensate tank flash	Methane, ethane, VOCs	MEET [24]	Condensate tank flash	Aggregated
	Water tank flash	Methane, ethane, VOCs	MEET [24]	Water tank flash	Aggregated
	Leaks	Methane, ethane, VOCs	MEET [24]	Varying compositions	Aggregated
	Pneumatic controllers	Methane, ethane, VOCs	MEET [24]	Produced gas	Aggregated
	Chemical injection pumps	Methane, ethane, VOCs	MEET [24]	Produced gas	Aggregated
	Heaters	Methane, ethane, VOCs, NOx	EPA Oil and Gas Tool [28]	County-throughput-produced gas composition and EPA Oil and Gas Tool	Aggregated
	Liquid unloadings	Methane, ethane, VOCs	MEET [24]	Produced gas	Not aggregated
Gathering and boosting	Total site emissions	Methane, ethane, VOCs, NOx	Zimmerle et al. [32]	Grid-cell-throughput-produced gas	Not applicable
Gas processing sites	Total site emissions	Methane, ethane, VOCs, NOx	GHGRP [19]	Grid-cell-throughput-produced gas	Not applicable
Gas transmission sites	Total site emissions	Methane, ethane, VOCs, NOx	GHGRP [19]	Grid-cell-throughput-produced gas	Not applicable
Flare	Flare emissions	Methane, ethane, VOCs, NOx	VIIRS [23]	Grid-cell-throughput-produced gas	Not applicable

Table 5. Activity data extracted and calculated from EPA GHGI for selected sources.

Simulated Source	Equipment	Unit	Dry Wells	Wet Wells	Oil Wells
Leaks	Meter/piping	Count per well	0.93		NA
Chemical injection pumps	Chemical injection pumps	Count per well	0.03	0.01	0
Pneumatic controllers	Pneumatic controllers	Count per well	0.97	0.63	0.29
	High bleed	Fraction	0.2%	0.1%	0%
	Low bleed	Fraction	17.3%	23.4%	43.8%
	Intermittent bleed	Fraction	82.5%	76.6%	56.7%
Heaters	Heaters	Count per well	0.1	0.06	0.02
Liquid unloading	Unloadings with plunger lifts	Fraction	4.0%		NA
	Unloadings without plunger lifts	Fraction	6.8%		NA

3. Results

Hourly emissions time series for methane, ethane, VOCs, and NOx are presented—aggregated at the grid cell, county, and basin level—in Figures 2–4. In Figures 2–4, emissions from well site preproduction activities, including drilling engines, hydraulic fracturing pumps, and completion flowbacks, were aggregated as the source category "comple-

tion/drilling/fracturing"; emissions from well site pneumatic controllers and chemical injection pumps were aggregated as the source category "pneumatic devices"; emissions from condensate tank flash and water tank flash at well sites were aggregated as "tank flash"; emissions from artificial lift engines, associated gas venting, heaters, and leaks on well sites were aggregated as "wellsite—other routine emissions"; emissions from gathering and boosting sites, gas processing sites, and transmission sites were aggregated as "gathering/processing/transmission"; emissions from flares and emissions from liquid unloadings on well sites were presented individually. Time series of emissions by individual source are available in the SI. Time series for additional grid cells and an additional county are presented in Supporting Information (SI). The selected grid cell presented in Figure 2 is located in Wetzel County, WV. It contained 70 actively producing wells in 2023, 11 of which were completed in 2023. Six wells were assigned liquid unloadings. Detailed well characteristics of selected grid cells are available in the SI.

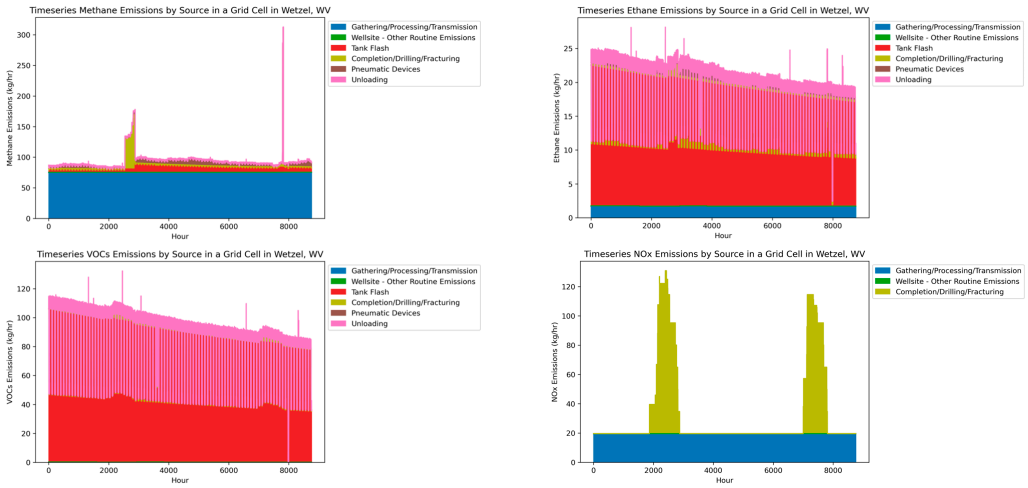

Figure 2. Hourly emissions time series for methane, ethane, VOC, and NOx emissions in a selected grid cell in Wetzel, WV.

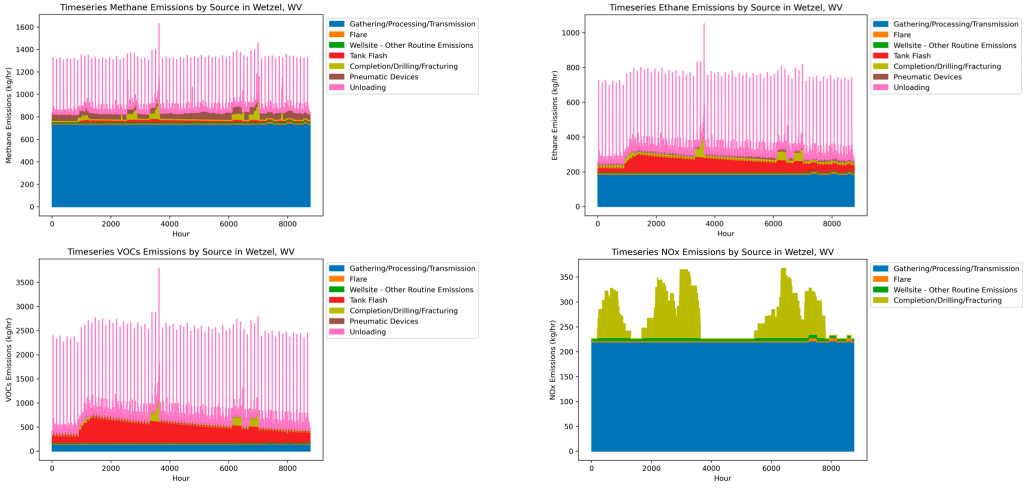

Figure 3. Hourly emissions time series for methane, ethane, VOC, and NOx emissions in Wetzel County, WV.

At the grid cell and the county level, though episodic emission sources such as liquid unloadings and preproduction activities dominate temporal variations in hydrocarbon emissions, total hydrocarbon emission rates generally decline as total production rates decline, and increase when total production rates increase, due to high initial production rates of the new wells completed. Such temporal declines were mainly driven by emissions

from tank flash and are consistent with the projected temporal evolution of methane emissions from oil and gas production sites [33]. Compared to methane emissions, ethane and VOC emissions showed a larger relative decline because tank flash emissions contribute to a higher fraction of ethane and VOCs' totals. However, at the basin level, such temporal declines were not observed because of the relatively stable production aggregated at the basin level.

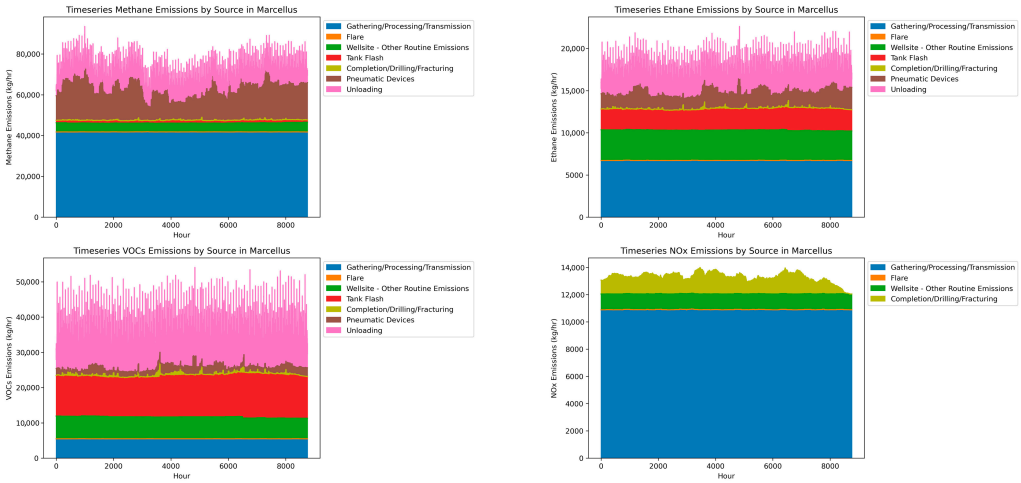

Figure 4. Hourly emissions time series for methane, ethane, VOC, and NOx emissions in the basin.

In Wetzel County, WV, methane emissions were primarily driven by gathering operations, with significant emission spikes from unloading events and occasional high-emission-rate completion events. Ethane and VOC emissions showed similar temporal patterns to those of methane, with greater contributions of emissions from condensate tank flashing. County-level ethane and VOC emissions from condensate tanks declined as existing wells aged and increased when new wells began production. In contrast, county-level methane emissions showed less sensitivity to this production change. Temporal variations in NOx emissions were driven by episodic, clustered drilling and fracturing events. In comparison, in Bradford County, PA, a dry gas production region with a comparable fraction of wells completed in 2023, temporal variability in total regional NOx emissions driven by preproduction activities was smoothed out due to the consistent high emissions from gathering operations. However, VOC emissions in Bradford were more significantly influenced by preproduction activities, in which drier gas was produced and no condensate tanks were present. Time series emissions in Bradford, PA, are available in the SI.

At the grid cell level, temporal variations in hydrocarbon emissions were primarily driven by liquid unloading and well completion events. In the absence of these events, emissions from pneumatic controllers also contributed to grid-level temporal variability (see SI Figures S4-2 and S4-6. NOx emissions were either relatively constant throughout the year or showed temporal variations driven by preproduction operations and flaring (see SI Figure S4-8).

At the basin level, spatial aggregation reduced the impact of intermittent events, especially for NOx emissions. Hydrocarbon emissions retained more temporal variations due to short, frequent, and high-rate events such as liquid unloadings and well completions. Pneumatic controllers, switching between low-emitting normal modes and high-emitting abnormal modes, also contributed to temporal variability at the basin level, particularly for methane and ethane.

Table 6 presents statistics of methane, ethane, VOC, and NOx emissions for the basin, Wetzel County, and the selected grid cell in Wetzel County, WV, as shown in Figure 2. Tables 7 and 8 summarize ratios of maximum to annual average hourly predicted emission

rates and the distribution of calculated ratios at various spatial levels. Additional summary tables for Bradford, PA, are available in the SI. Maximum to average emission rate ratios decreased as the scale of spatial aggregation increased because spatial aggregation masks emissions intermittency. For example, the ratio of maximum to average emission rate for VOC emissions was 1.6 at the basin level and 5.8 in Wetzel County. At the grid cell level, this ratio exceeded 100 in some grid cells within Wetzel County, WV. Compared to hydrocarbon emissions, NOx emissions presented less temporal variability in most counties, since NOx emissions were dominated by continuous emissions from gathering, processing, and transmission sites at most times. Exceptions are in the counties with little current production but with occasional preproduction activities for new wells. In these counties, NOx emissions were dominated by episodic emissions from preproduction activities and showed greater temporal variations. Maximum to average ratio for NOx emission rates was 1.1 and 1.4 at the basin level, and in Wetzel County, WV, respectively. The sources driving temporal variability for hydrocarbon emissions were liquid unloadings and well completions, while the sources driving temporal variability in NOx emissions were preproduction activities such as drilling and hydraulic fracturing. At finer spatial scales such as the grid cell level, NOx emissions from flares can also lead to elevated emission rates (see SI).

Table 6. Distributions of methane, ethane, VOC, and NOx emission rates for the basin, Wetzel County, and the selected grid cell.

Emission Rates Statistics (kg/h)	Mean	Median	75%	90%	Max
		Basin			
Methane	69,822	69,902	72,811	76,098	93,545
Ethane	16,885	16,668	17,346	18,375	22,613
VOCs	33,898	32,645	35,104	39,678	54,081
NOx	13,300	13,331	13,540	13,709	13,997
		Wetzel County, WV			
Methane	860	843	864	898	1629
Ethane	307	300	323	341	1051
VOCs	651	631	731	803	3796
NOx	272	266	317	337	368
		Selected grid cell in Wetzel County, WV			
Methane	94	91	96	98	313
Ethane	19	20	22	23	28
VOCs	83	90	100	107	132
NOx	34	20	20	95	131

Table 7. Ratios of maximum to annual average hourly predicted emission rates at the basin and county levels and distributions of the ratios among 173 counties included in the basin.

Emissions	Basin	Wetzel, WV, USA	Bradford, PA, USA	Distribution of Ratios Among 173 Counties						
				Mean	Std	Min	25%	50%	75%	Max
Methane	1.3	1.9	1.6	3.3	2.5	1.0	1.7	2.7	3.7	18
Ethane	1.3	3.4	1.6	3.5	2.5	1.0	2.0	2.8	3.9	18
VOCs	1.6	5.8	2.5	5.3	6.2	1.0	2.2	3.6	5.5	41
NOx	1.1	1.4	1.2	1.3	0.8	1.0	1.0	1.0	1.3	9.3

Table 8. Ratios of maximum to annual average hourly predicted emission rates at a selected grid cell level and distributions of the ratios among 36 grid cells located within Wetzel County, WV.

Emissions	Selected Grid Cell	Distribution of Ratios Among 36 Grid Cells in Wetzel, WV, USA						
		Mean	Std	Min	25%	50%	75%	Max
Methane	3.4	3.5	4.3	1.0	1.2	1.7	4.0	24
Ethane	1.4	5.2	6.0	1.1	1.3	2.6	6.1	29
VOCs	1.5	15	24	1.1	1.8	3.7	19	126
NOx	6.7	1.9	2.1	1.0	1.0	1.0	1.0	8.4

4. Discussion

Although this work focuses on the Marcellus basin, the simulation framework and methods developed in this work can be broadly applied in other oil and gas production regions. Temporal variations in emissions may change depending on production characteristics in the region. For example, in the Permian Basin where the majority of wells are oil producing wells, fewer emissions from liquid unloadings occur [34] and less temporal variations are expected. The ability to simulate temporally resolved emissions at various spatial levels is important in basins with varying production characteristics. For example, the Eagle Ford Shale has subregions with distinct production profiles, ranging from oil-dominated regions to wet gas and dry gas production regions [35]. Basin-level estimates cannot accurately represent the emission characteristics in sub-regions within the basin. Dominant emission sources and temporal variations in emissions vary within the basin. The sources that dominate temporal variations in emissions vary by pollutant, and results from this work are consistent with prior published measurements and inventories. For example, a top-down/bottom-up methane emission reconciliation study reported that episodic emissions from manual liquid unloadings drive temporal variations in the basin-level emission rates by a factor of two [14].

Methods for reconciling these predicted time series with measurements will vary depending on the intermittency in emissions predicted and the type of measurement being made. For example, satellite or aircraft measurements could be made to estimate total area-wide emissions at the scale of a county or basin. In these cases, if emissions are relatively constant over the time-scale of a day, such as for NOx, then the average emission estimate for the day could be compared to the instantaneous measurement made by a satellite or an aircraft performing a mass balance flight. There is, however, day-to-day variability in emissions, and in the case study considered in this work, that day-to-day variability at a county level can be 20% or more.

Reconciliations between predicted emission inventory time series and observations are more complex when emissions have durations of less than a day or have a diurnal pattern. This is the case for unloading emissions in the Marcellus region. Consider a county with 1000 wells (similar to Wetzel County), where 10% of the liquid unloadings lead to venting, and each well vents 10 times per year. This would lead to an expected value of 1000 venting events per year. If the venting was distributed evenly throughout the day, then three unloadings would be expected on any day. In contrast, if the unloadings only occur during an 8 h working period, nine unloadings would be expected in each working day, when measurements from aircraft and satellites are typically made. If the unloadings were distributed uniformly throughout the working day, and each lasted slightly less than an hour, then at any given time during the working day, one unloading should be observed in a county. In contrast, if unloadings were distributed uniformly throughout the day, then only on one day in three would an hour-long unloading be observed during an instantaneous

measurement in the hypothetical county. If the duration of the events was 30 min instead of an hour, the expected frequency for observing unloadings would be cut in half.

These simple examples illustrate the care that must be taken in comparing predicted intermittent, short duration events with observations. Accurate comparisons will depend on the frequency, duration, and diurnal patterns of the emission events [15]. For large emission rates such as blowdowns or unloadings, a single event at a single site can have a significant impact on the instantaneous emission rates at the scale of a basin or county [14]. Emission predictions, accounting for emission intermittency and diurnal variations, should be compared to observations at the time that measurements are made.

5. Conclusions

Hourly emissions of methane, ethane, VOCs, and NOx were estimated for the calendar year 2023 across more than 200,000 well sites in the Marcellus oil and gas production region. Emissions were aggregated in terms of 4 km-by 4-km grid cells, counties, and the basin. Temporal variability in emissions increased at finer levels of spatial aggregation and varied by pollutant. Hydrocarbon emissions, dominated by episodic events such as liquid unloadings, have larger temporal variations compared to NOx emissions, which are dominated by combustion sources with relatively consistent emission rates. The sources that drive temporal variations in hydrocarbon emissions were liquid unloadings, whereas the sources that drive temporal variations in NOx emissions were drilling and fracturing activities.

The framework presented in this work is broadly applicable in other oil and gas production regions, and the ability to simulate temporally and spatially resolved inventories enables the development of pollutant- and region-specific measurement campaigns and mitigation strategies. Reconciliation between predicted inventory and measurements requires accounting for the frequency, duration, and time-of-day variability in emissions, as well as the spatial scale and timing of the observations.

Supplementary Materials: The following supporting information can be downloaded at: https://www.mdpi.com/article/10.3390/atmos16091048/s1, S1: production data; S2: selected grid cells; S3: emission sources and simulation methods; S4: base case analyses; S5: sensitivity analyses [9,19,21,23,24,26,28–30,32,36–41].

Author Contributions: Conceptualization, D.T.A.; methodology, Q.C.; software, Q.C., N.R., L.N. and S.J.A.; validation, Q.C., J.D.G. and V.B.; formal analysis, Q.C.; investigation, Q.C.; resources, D.T.A.; data curation, Q.C. and S.S.; writing—original draft preparation, Q.C. and D.T.A.; writing—review and editing, Q.C., J.D.G., D.T.A. and L.H.R.; visualization, Q.C.; supervision, D.T.A.; project administration, D.T.A., S.S., Q.C. and L.H.R.; funding acquisition, D.T.A. and L.H.R. All authors have read and agreed to the published version of the manuscript.

Funding: Research described in this work was conducted under contract to the Health Effects Institute (HEI), an organization jointly funded by the United States Environmental Protection Agency (EPA) (contract no. 68HERC19D0010) and certain oil and natural gas companies. Although the research was produced with partial funding by the EPA and industry, they have not been subject to review, and therefore, the research does not necessarily reflect the views of the agency or the oil and natural gas industry, and no official endorsement by the agency or the industry should be inferred.

Institutional Review Board Statement: Not applicable.

Informed Consent Statement: Not applicable.

Data Availability Statement: The original data presented in the study are openly available at: https://www.ceesa.utexas.edu/.

Conflicts of Interest: D.T.A. and L.H.R. have served on the Environmental Protection Agency's Science Advisory Board; in this role, they were paid Special Governmental Employees. D.T.A.'s research is

currently supported by the National Science Foundation, the Department of Energy, the Texas Commission on Environmental Quality, Chevron, ExxonMobil, Pioneer Natural Resources, and the Environmental Defense Fund. He has also worked on projects that have been supported by oil and gas producers and the Environmental Defense Fund. D.T.A. has worked as a consultant for multiple companies, including Cheniere, Eastern Research Group, KeyLogic, and SLR International. L.H.R.'s research is currently supported by the Texas Commission on Environmental Quality, the Health Effects Institute, the Welch Foundation, and ExxonMobil. In the summer of 2025, J.D.G. was a consultant for the United Nations Environment Programme's International Methane Emissions Observatory, working on the Oil and Gas Methane Partnership 2.0. L.N. was an intern at Baker Hughes.

References

1. Allen, D.T.; Cardoso-Saldaña, F.J.; Kimura, Y. Variability in Spatially and Temporally Resolved Emissions and Hydrocarbon Source Fingerprints for Oil and Gas Sources in Shale Gas Production Regions. *Environ. Sci. Technol.* **2017**, *51*, 12016–12026. [CrossRef]
2. National Petroleum Council. Charting the Course. Available online: https://chartingthecourse.npc.org/documents/Charting_the_Course-V2-FINAL.pdf?a=1739340884 (accessed on 9 July 2025).
3. Zavala-Araiza, D.; Alvarez, R.A.; Lyon, D.R.; Allen, D.T.; Marchese, A.J.; Zimmerle, D.J.; Hamburg, S.P. Super-emitters in natural gas infrastructure are caused by abnormal process conditions. *Nat. Commun.* **2017**, *8*, 14012. [CrossRef] [PubMed]
4. Omara, M.; Zimmerman, N.; Sullivan, M.R.; Li, X.; Ellis, A.; Cesa, R.; Subramanian, R.; Presto, A.A.; Robinson, A.L. Methane Emissions from Natural Gas Production Sites in the United States: Data Synthesis and National Estimate. *Environ. Sci. Technol.* **2018**, *52*, 12915–12925. [CrossRef] [PubMed]
5. Alvarez, R.A.; Zavala-Araiza, D.; Lyon, D.R.; Allen, D.T.; Barkley, Z.R.; Brandt, A.R.; Davis, K.J.; Herndon, S.C.; Jacob, D.J.; Karion, A.; et al. Assessment of methane emissions from the US oil and gas supply chain. *Science* **2018**, *361*, 186–188. [CrossRef]
6. Macey, G.P.; Breech, R.; Chernaik, M.; Cox, C.; Larson, D.; Thomas, D.; Carpenter, D.O. Air concentrations of volatile compounds near oil and gas production: A community-based exploratory study. *Environ. Health* **2014**, *13*, 82. [CrossRef]
7. Allen, D.T. Emissions from oil and gas operations in the United States and their air quality implications. *J. Air Waste Manag. Assoc.* **2016**, *66*, 549–575. [CrossRef]
8. Dix, B.; Francoeur, C.; Li, M.; Serrano-Calvo, R.; Levelt, P.F.; Veefkind, J.P.; McDonald, B.C.; de Gouw, J. Quantifying NO_x Emissions from U.S. Oil and Gas Production Regions Using TROPOMI NO_2. *ACS Earth Space Chem.* **2022**, *6*, 403–414. [CrossRef]
9. Modi, M.; Kimura, Y.; Ruiz, L.H.; Allen, D.T. Fine Scale Spatial and Temporal Allocation of NOx Emissions from Unconventional Oil and Gas Development Can Result in Increased Predicted Regional Ozone Formation. *ACS EST Air* **2024**, *2*, 130–140. [CrossRef]
10. Johnson, D.; Heltzel, R.; Oliver, D. Temporal Variations in Methane Emissions from an Unconventional Well Site. *ACS Omega* **2019**, *4*, 3708–3715. [CrossRef]
11. Johnson, D.; Heltzel, R. On the Long-Term Temporal Variations in Methane Emissions from an Unconventional Natural Gas Well Site. *ACS Omega* **2021**, *6*, 14200–14207. [CrossRef] [PubMed]
12. Wang, J.L.; Daniels, W.S.; Hammerling, D.M.; Harrison, M.; Burmaster, K.; George, F.C.; Ravikumar, A.P. Multiscale Methane Measurements at Oil and Gas Facilities Reveal Necessary Frameworks for Improved Emissions Accounting. *Environ. Sci. Technol.* **2022**, *56*, 14743–14752. [CrossRef]
13. Daniels, W.S.; Wang, J.L.; Ravikumar, A.P.; Harrison, M.; Roman-White, S.A.; George, F.C.; Hammerling, D.M. Toward Multiscale Measurement-Informed Methane Inventories: Reconciling Bottom-Up Site-Level Inventories with Top-Down Measurements Using Continuous Monitoring Systems. *Environ. Sci. Technol.* **2023**, *57*, 11823–11833. [CrossRef]
14. Vaughn, T.L.; Bell, C.S.; Pickering, C.K.; Schwietzke, S.; Heath, G.A.; Pétron, G.; Zimmerle, D.J.; Schnell, R.C.; Nummedal, D. Temporal variability largely explains top-down/bottom-up difference in methane emission estimates from a natural gas production region. *Proc. Natl. Acad. Sci. USA* **2018**, *115*, 11712–11717. [CrossRef] [PubMed]
15. Huang, L.; Stokes, S.; Chen, Q.; Allen, D.T. Uncertainties in the Estimated Methane Emissions in Oil and Gas Production Regions Based on Aircraft Mass Balance Flights. *Chem. Eng.* **2024**, *12*, 11024–11032. [CrossRef]
16. Schissel, C.; Allen, D.T. Impact of the High-Emission Event Duration and Sampling Frequency on the Uncertainty in Emission Estimates. *Environ. Sci. Technol. Lett.* **2022**, *9*, 1063–1067. [CrossRef]
17. U.S. Environmental Protection Agency (EPA). Inventory of U.S. Greenhouse Gas Emissions and Sinks. Available online: https://www.epa.gov/ghgemissions/inventory-us-greenhouse-gas-emissions-and-sinks (accessed on 11 September 2022).
18. U.S. Environmental Protection Agency. National Emissions Inventory (NEI). Available online: https://www.epa.gov/air-emissions-inventories/national-emissions-inventory-nei (accessed on 12 August 2025).
19. U.S. Environmental Protection Agency. EPA Facility Level GHG Emissions Data. Available online: https://ghgdata.epa.gov/ghgp/main.do (accessed on 9 July 2025).

20. Texas Commission on Environmental Quality. Point Source Emissions Inventory. Available online: https://www.tceq.texas.gov/airquality/point-source-ei (accessed on 12 August 2025).
21. Enverus. Available online: https://prism.enverus.com/prism/home (accessed on 3 November 2024).
22. Esri. World Imagery. Available online: https://services.arcgisonline.com/ArcGIS/rest/services/World_Imagery/MapServer (accessed on 10 July 2025).
23. Earth Observation Group. Global Gas Flaring Observed from Space. Available online: https://eogdata.mines.edu/products/vnf/global_gas_flare.html (accessed on 8 July 2025).
24. Allen, D.T.; Cardoso-Saldaña, F.J.; Kimura, Y.; Chen, Q.; Xiang, Z.; Zimmerle, D.; Bell, C.; Lute, C.; Duggan, J.; Harrison, M. A Methane Emission Estimation Tool (MEET) for predictions of emissions from upstream oil and gas well sites with fine scale temporal and spatial resolution: Model structure and applications. *Sci. Total Environ.* **2022**, *829*, 154277. [CrossRef]
25. Cardoso-Saldaña, F.J.; Pierce, K.; Chen, Q.; Kimura, Y.; Allen, D.T. A Searchable Database for Prediction of Emission Compositions from Upstream Oil and Gas Sources. *Environ. Sci. Technol.* **2021**, *55*, 3210–3218. [CrossRef] [PubMed]
26. Allen, D.T.; Torres, V.M.; Thomas, J.; Sullivan, D.W.; Harrison, M.; Hendler, A.; Herndon, S.C.; Kolb, C.E.; Fraser, M.P.; Hill, A.D.; et al. Measurements of methane emissions at natural gas production sites in the United States. *Proc. Natl. Acad. Sci. USA* **2013**, *110*, 17768–17773. [CrossRef] [PubMed]
27. Colón, Y.A.R.; Ruppert, L.F. *Central Appalachian Basin Natural Gas Database: Distribution, Composition, and Origin of Natural Gases*; USGA: Reston, VA, USA, 2015. [CrossRef]
28. U.S. Environmental Protection Agency. 2020 Nonpoint Oil and Gas Emissions Estimation Tool V1.3. Available online: https://gaftp.epa.gov/Air/nei/2020/doc/supporting_data/nonpoint/oilgas/OIL_GAS_TOOL_v1.3/ (accessed on 9 July 2025).
29. U.S. Environmental Protection Agency. Inventory of U.S. Greenhouse Gas Emissions and Sinks: 1990–2022. Available online: https://www.epa.gov/ghgemissions/inventory-us-greenhouse-gas-emissions-and-sinks-1990-2022 (accessed on 9 July 2025).
30. U.S. Environmental Protection Agency. AP-42: Compilation of Air Emissions Factors from Stationary Sources. Available online: https://www.epa.gov/air-emissions-factors-and-quantification/ap-42-compilation-air-emissions-factors-stationary-sources (accessed on 9 July 2025).
31. Graves, J.D.; Kimura, Y.; Modi, M.; Stokes, S.; Meyer, M.; Ruiz, L.H.; Allen, D.T. Source Attribution of Elevated Ethane Concentrations Detected by Regional Monitors in Oil and Gas Production Regions. *ACS EST Air* **2025**. [CrossRef]
32. Vaughn, T.; Luck, B.; Lauderdale, T.; Keen, K.; Harrison, M.; Marchese, A.J.; Williams, L.L.; Allen, D.T. Methane Emissions from Gathering Compressor Stations in the U.S. *Environ. Sci. Technol.* **2020**, *54*, 7552–7561. [CrossRef]
33. Cardoso-Saldaña, F.J.; Allen, D.T. Projecting the Temporal Evolution of Methane Emissions from Oil and Gas Production Sites. *Environ. Sci. Technol.* **2020**, *54*, 14172–14181. [CrossRef] [PubMed]
34. Zaimes, G.G.; Littlefield, J.A.; Augustine, D.J.; Cooney, G.; Schwietzke, S.; George, F.C.; Lauderdale, T.; Skone, T.J. Characterizing Regional Methane Emissions from Natural Gas Liquid Unloading. *Environ. Sci. Technol.* **2019**, *53*, 4619–4629. [CrossRef] [PubMed]
35. Gherabati, S.A.; Browning, J.; Male, F.; Ikonnikova, S.A.; McDaid, G. The impact of pressure and fluid property variation on well performance of liquid-rich Eagle Ford shale. *J. Nat. Gas Sci. Eng.* **2016**, *33*, 1056–1068. [CrossRef]
36. ENVIRON International Corporation and Inc. Eastern Research Group. 2011 Oil and Gas Emission Inventory Enhancement Project for CenSARA States. Available online: https://www.arb.ca.gov/ei/areasrc/oilandgaseifinalreport.pdf (accessed on 9 July 2025).
37. Eastern Research Group, Inc. Specified Oil & Gas Well Activities Emissions Inventory Update Prepared for: Texas Commission on Environmental Quality Air Quality Division. Available online: https://wayback.archive-it.org/414/20210527185258/https://www.tceq.texas.gov/assets/public/implementation/air/am/contracts/reports/ei/5821199776FY1426-20140801-erg-oil_gas_ei_update.pdf (accessed on 9 July 2025).
38. Allen, D.T.; Pacsi, A.P.; Sullivan, D.W.; Zavala-Araiza, D.; Harrison, M.; Keen, K.; Fraser, M.P.; Hill, A.D.; Sawyer, R.F.; Seinfeld, J.H. Methane Emissions from Process Equipment at Natural Gas Production Sites in the United States: Pneumatic Controllers. *Environ. Sci. Technol.* **2015**, *49*, 633–640. [CrossRef]
39. Energy Information Administration. Natural Gas Monthly Report. Available online: https://www.eia.gov/naturalgas/monthly/ (accessed on 8 July 2025).
40. Allen, D.T.; Sullivan, D.W.; Zavala-Araiza, D.; Pacsi, A.P.; Harrison, M.; Keen, K.; Fraser, M.P.; Hill, A.D.; Lamb, B.K.; Sawyer, R.F.; et al. Methane Emissions from Process Equipment at Natural Gas Production Sites in the United States: Liquid Unloadings. *Environ. Sci. Technol.* **2015**, *49*, 641–648. [CrossRef]
41. Vaughn, T.L.; Luck, B.; Williams, L.; Marchese, A.J.; Zimmerle, D. Methane Exhaust Measurements at Gathering Compressor Stations in the United States. *Environ. Sci. Technol.* **2021**, *55*, 1190–1196. [CrossRef]

Supplementary Materials:

Qining Chen, Nadin Raksi, Lily Niewenhous, Sewar Almasalha, Joel D. Graves, V'Jae Brown, Shannon Stokes, David T. Allen *, and Lea Hildebrandt Ruiz

S1. Production data

Production data downloaded from the Enverus database [21] report the total production over the past 12 months for each well. The exact definition of "past 12 months" varies by well depending on the last reporting date of the well, but generally falls within the 2023 calendar year. For simplicity, we assume the reported production data represent annual production for 2023. Table S1-1 summarizes annual production rate aggregated in the basin and the two selected counties.

Table S1. Annual production from wells included in simulation aggregated in the basin and the two selected counties.

	Active well counts	Gas production (BCF/year)	Oil production (MMBBL/year)	Water production (MMBBL/year)	Gas-to-oil ratio (SCF/BBL)
Basin level	201338	12658	49	139	255875
Bradford, PA	1520	1089	0	3.0	NA
Wetzel, WV	1295	483	1.3	7.2	375000

Daily production rates and well ages at the beginning of the simulation, as of January 1, 2023, were calculated on a well-by-well basis and combined with decline curves to determine the production decline throughout 2023. For wells completed before 2023, daily production rate at the beginning of the simulation was estimated by dividing the reported annual production by 12 months and then by 30 days. Well age at the beginning of the simulation was calculated as the time difference between the well completion date and the simulation start date. For wells completed in 2023, the initial production rate was calculated as the daily average of "first three months production", as reported in the Enverus database [21]. For these wells, production declines and emissions simulation associated with production activities start after the completion date.

S2. Selected grid cells

As described in the main text, in the two selected counties, Bradford, PA and Wetzel, WV, emissions were aggregated at the grid cell level. Four grid cells, two from each county, were selected to present the grid-level simulations. Locations of the selected grid cells are shown in Figure S2-1. Well types and production distributions in the selected grid cells are reported in Tables S2-1 and S2-2.

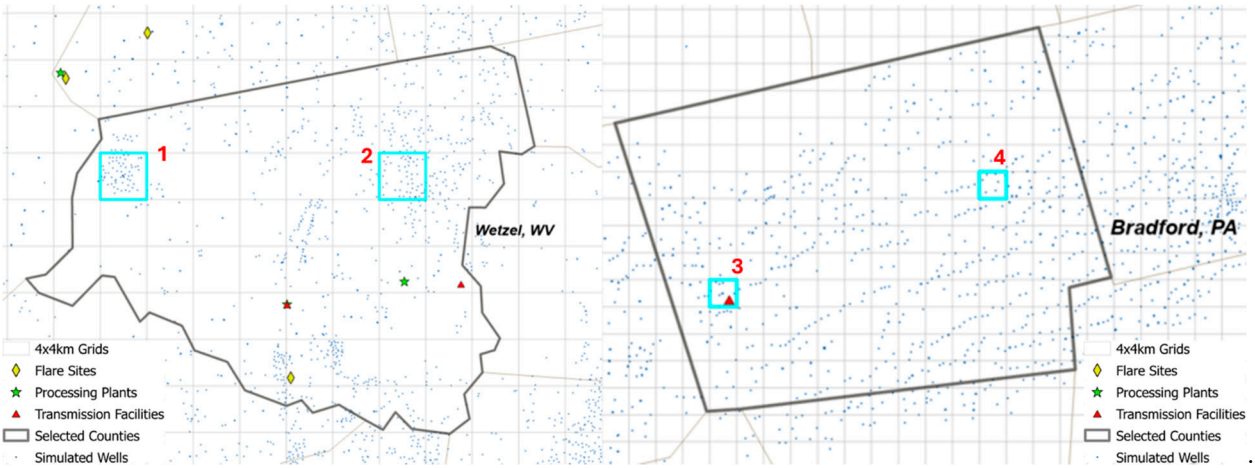

Figure S2. Locations of the 4 selected grid cells in Wetzel, WV and Bradford, PA. Each grid cell measures 4 km by 4 km. Grid cell 3 in Bradford County has a transmission facility.

Table S2. Distributions of simulated wells in selected grid cells.

Grid cell	Total count of wells	Horizontal /directional	Vertical	Dry gas[1]	Wet gas[2]	Oil[3]	Wells completed in 2023	Wells with liquid unloadings with plunger	Wells with liquid unloadings without plunger
1	83	29	54	37	46	0	0	0	0
2	70	26	44	47	22	1	11	2	4
3	42	42	0	42	0	0	0	0	0
4	9	9	0	9	0	0	0	0	0

[1] Dry gas wells are wells with <1% liquids production in wellhead stream.

[2] Wet gas wells include wells classified as wet gas wells (1-10% liquids in wellhead stream) and liquid rich gas wells (10-40% liquids in wellhead stream).

[3] Oil wells are wells with >40% liquids production in wellhead stream.

Table S2. Annual production in selected grid cells.

Grid cell	Gas production (MCF/year)	Oil production (BBL/year)	Water production (BBL/year)	Gas-to-oil ratio (SCF/BBL)
1	5606576	17709	18327	316595
2	75731756	217513	796282	348171
3	4167280	0	5698	NA
4	661934	0	3130	NA

S3. Emission sources and simulation methods

S3.1. Drilling engines

Drilling engines emissions were estimated for wells drilled and completed in 2023. Well drilling was assumed to start 4 weeks before the well completion date and last for 2 weeks. Methane, VOCs, and NOx emissions from drilling engines were estimated using the EPA Oil and Gas Tool [28]. The 2020 version was the most recent version with complete documentation. Table S3-1 reports total drilling emissions per drilling depth, calculated with the activity factors and emission factors of drilling engines specific to the

Marcellus. Total drilling emissions per drilling depth were then combined with drilling depth per well, to estimate total drilling emissions per well. Total drilling emissions per well were temporally allocated over the two-week drilling period, with emission rates evenly distributed. Ethane emissions were considered negligible, assuming drilling engines were all diesel engines, according to data reported in the EPA Oil and Gas Tool. Drilling emissions were always simulated at the well level, regardless of the spatial scales of post aggregation and reporting, as the timing of drilling events varied by well.

Table S3-1. Total drilling emissions per drilling depth from drilling engines.

Well type	Methane, kg per meter drilled	VOCs, kg per meter drilled	NOx, kg per meter drilled
Horizontal	0.83	0.036	0.0029
Vertical	0.26	0.014	0.0014

S3.2. Hydraulic fracturing pumps

Hydraulic fracturing pumps emissions were estimated for the wells fractured and completed in 2023. Hydraulic fracturing was assumed to occur during the 2 weeks prior to the well completion date, immediately following the end of drilling activities. Methane, VOCs, and NOx emissions per event were estimated with the activity factors and emission factors of hydraulic fracturing pump engines specific to Marcellus, available in the EPA Oil and Gas Tool [28]. Per-event emissions were temporally allocated to the two-week hydraulic fracturing period with emission rates evenly distributed. Ethane emissions were considered negligible, assuming all fracturing pumps used diesel fuel. Fracturing emissions were always simulated at the well level due to different fracturing timings per well.

Emission factors per event and emission rates after temporal allocation are reported in Table S3-2. Two sets of activity and emission factors were available in the EPA Oil and Gas Tool. The EPA default factors were sourced from an inventory developed based in seven states including Louisiana, Oklahoma, Arkansas, Kansas, Missouri and Nebraska [36]. EPA default factors are significantly lower than fracturing emissions factors reported elsewhere in the literature [9]. An alternative set of factors developed for Texas basins [37], resulted in per-event emissions approximately 40 times higher than those estimated with the EPA defaults. While no detailed, region-specific study has been done in the Marcellus, the alternative factors developed for Texas basins were considered a more accurate estimate and were used in the base case simulation. The EPA default factors were applied in a sensitivity scenario.

Table S3-2. Total hydraulic fracturing pumps emissions per fracturing event.

Factor scenarios	Unit	Methane	VOCs	NOx
EPA defaults	Total emissions per event (kg)	0.37	5.1	127
	Emission rate (kg/hr)	0.0011	0.015	0.38
Alternative factors developed for Texas basins – used in the base case simulation	Total emissions per event (kg)	15	203	5082
	Emission rate (kg/hr)	0.045	0.61	15

S3.3. Completion flowbacks

Completion flowbacks emissions were estimated for wells completed in 2023 using the Methane Emission Estimation Tool (MEET) [24]. Completions were simulated as two-stage events, with varying durations and methane emission rates sampled from distribution of measurements [26]. Ethane and VOCs emission rates were estimated based on methane emission rates and wellstream compositions per well. Completion emissions were always simulated at the well level due to different timings of events at individual wells.

S3.4. Artificial lift engines

Artificial lift engines are deployed at oil wells to lift liquids from the wellbore to the wellhead. Assuming one artificial lift engine per oil well, artificial lift engine emissions scale linearly with the number of oil wells at each spatial scale. In the two selected counties, these emissions were simulated at the grid cell level, and for the entire basin, these emissions were simulated at the county level. Methane, VOCs, and NOx emissions were estimated based on state-specific activity factors and emission factors of the engines, extracted from the EPA Oil and Gas Tool [28]. Although individual artificial lift engines may cycle on and off depending on their operating hours, total emission rates at the grid cell or the county level were assumed to be constant throughout the simulation period. Calculated emission rates were normalized by average annual operating hours to account for the intermittent operation of individual engines. State-specific average emission rates per oil well are reported in Table S3-3. Ethane emissions were estimated based on methane emissions and the ethane-to-methane composition ratio in throughput gas at the county level.

Table S3-3. State-specific average emission rates per oil well from artificial lift engines.

State	Methane, kg/hr/well	VOCs, kg/hr/well	NOx, kg/hr/well
KY	4.53e-03	5.83e-04	4.47e-02
NY	1.59e-06	2.04e-07	1.57e-05
OH	5.86e-05	7.54e-06	5.78e-04
PA	4.53e-03	5.83e-04	4.47e-02
VA	4.53e -03	5.83e-04	4.47e-02
WV	4.53e -03	5.83e-04	4.47e-02

S3.5. Associated gas venting

Associated gas venting emissions scale linearly with the number of oil wells at each spatial scale. In the two selected counties, these emissions were simulated at individual oil wells, and for the entire basin, these emissions were simulated per aggregated oil well per county after pre-simulation aggregation. The gas venting rate per oil production was estimated as a constant value of 0.15 MCF per barrel of oil produced and was assumed uniform across the basin [28]. Emissions due to flaring controls were not counted under associated gas venting to avoid double counting. Flaring activities were assumed to be captured by satellite with associated emissions counted under flare emissions.

S3.6. Condensate tank flash

The assignment of condensate tank counts per well depends on oil production rates. Condensate tank flash emissions were simulated if the well has non-zero oil production. In the two selected counties, tank emissions were simulated at the well level. Methane and ethane emissions due to tank flash were simulated with MEET at hour resolution and emission rates declined as production declined over time. Summed propane and butane emissions were used as a surrogate for VOC emissions. The production decline per well

was simulated based on the well-specific completion date, production data, and hyperbolic decline parameters drawn from a location-based decline parameter database built in the MEET model . Tanks at well sites with oil production were assumed with emission controls at 95% efficiency on both oil and water tanks, whereas tanks at sites with no oil production had no tank controls applied.

For the basin-level simulation, a pre-simulation aggregation step is involved, which aggregates wells of the same production type into an aggregated well per county. At the aggregated well, tank emissions were first simulated at a constant rate, based on a constant production rate from the wells being aggregated, without considering production declines. Then, two sets of scaling factors, a production scaling factor and a control scaling factor, were developed, accounting for county-level production declines and emission controls. The final emissions at each hour were calculated by multiplying the time series scaling factors with the constant tank emissions output from MEET.

The production scaling factor accounts for production declines over time and assumes tank emission rates change linearly with production rates. Time series of hourly production was simulated for each well based on its specific completion date and current production rate, using a hyperbolic decline model specific to each county. The simulated hourly production was then aggregated by county to develop a time series of production scaling factors. This set of factors are defined as the ratios of actual aggregated production to the constant aggregated production used in the MEET simulation.

The control scaling factor adjusts for the proportion of liquid production under control. A 95% control rate was applied to oil-producing wells. Hourly liquid production was simulated per well, and controlled versus uncontrolled production was aggregated by county and by hour. The control factor is calculated as the ratio of the liquid production from controlled wells to the total liquid production within the aggregation.

S3.7. Water tank flash

Water tank flash emissions were simulated using the same method as condensate tank flash emissions, based on water production.

S3.8. Leaks

Leaks were simulated by MEET through leak / no-leak transitions per leaking component from wellhead, separator, tanks, and meter/piping. Each well was assigned one wellhead. The count of separators assigned depends on the number of phases in production: if the well produces both gas and liquids, one separator is assigned; if the well produces only gas or only liquids, no separator is assigned. The number of tanks assigned per well depends on the existence of oil and water production per well as described above. Meter/piping was randomly assigned to gas wells classified as dry gas wells and wet gas wells. Dry and wet gas wells have either 1 or 0 meter/piping assigned per well, with an average of 0.93 counts per well, while oil wells have no meter/piping assigned. Emission rates per leaking component were drawn from the distribution of measured emissions in the literature [26].

S3.9. Chemical injection pumps

Chemical injection pumps were randomly assigned to wells as either 0 or 1 per well, based on the average count per well type, as shown in Table 5 in the main text. Emissions from chemical injection pumps were simulated by MEET. Emission rates were drawn

from distribution of measured emissions [26] and were constant throughout the simulation.

In the two selected counties, chemical injection pump emissions were simulated at the individual well level. For the basin-level simulation, emissions were modeled at the level of aggregated wells per county. Although the total number of chemical injection pumps assigned to an aggregated well equals the sum of pump from all wells being aggregated into this aggregated well, only a single pump was simulated per aggregated well. The emissions from this single simulated pump were then scaled by the total pump count to estimate emissions from chemical injection pumps for the aggregated well.

S3.10. Pneumatic controllers

Pneumatic controllers were randomly assigned to wells, based on the average count per well type and the fraction per controller type, as shown in Table 5 in the main text. The fractions of each type of pneumatic controllers for wet gas wells were calculated using a weighted average based on the total pneumatic controller counts for dry and oil wells. Emissions from pneumatic controllers were simulated by MEET. Simulations transitioned between normal and abnormal operating modes, with normal and abnormal emission factors drawn from distribution of measured emissions [38]. For basin level simulation, emissions were simulated and scaled using the same method as for chemical injection pumps.

S3.11. Heaters

Heater emissions scale linearly with the number of heaters in spatial aggregation. Heaters were randomly assigned to wells based on the average number of heaters per well, as shown in Table 5 in the main text. Each well was assigned either one heater or none. Heaters were assumed to operate continuously throughout the year with constant emission rates. Methane, VOCs, and NOx emissions from heaters were estimated by combining basin-wide heater emission factors per volume of gas combusted and heater rated energy input, available in the EPA Oil and Gas Tool, with state-specific heating values of natural gas in 2023 reported by U.S. Energy Information Administration [39]. Heating values of combusted natural gas and calculated heater emission rates per state are reported in Table S3-4.

Table S3-4. Heating values of combusted natural gas and calculated heater emission rates per heater per state.

State	Heating values, BTU/SCF	Methane, kg/hr/heater	VOC, kg/hr/heater	NOx, kg/hr/heater
PA	1036	6.48e-04	1.55e-03	1.64e-02
WV	1082	6.20e-04	1.48e-03	1.57e-02
KY	1055	6.36e-04	1.52e-03	1.61e-02
NY	1032	6.50e-04	1.55e-03	1.65e-02
OH	1066	6.29e-04	1.51e-03	1.59e-02
VA	1050	6.39e-04	1.53e-03	1.62e-02

S3.12. Liquid unloadings

Liquid unloading emissions were always simulated at individual well level due to well specific timings of emissions. Liquid unloading operations were assigned to a subset of gas wells with nonzero gas production, completed in and before 2020, and with lowest gas-to-liquids producing ratios. As shown in Table 5 in the main text, a total of 11% of

wells across the basin were assigned liquid unloading operations with or without plunger lifts. Number of wells assigned liquid unloadings at the basin and the county levels are reported in Table S3-5. There is limited publicly available information on whether the unloadings with plunger lifts are manual or automated. In the base case simulation, all liquid unloadings with plunger lifts were assumed to be automated. Manual unloadings of wells without plunger lifts and automated unloadings with plunger lifts were assigned randomly among the wells with liquid unloadings, based on the fraction of each unloading technology shown in Table 5 in the main text. Activity and emission data for unloading events per well were randomly drawn from field measurements [40]. Compared to automated unloading operations, manual unloading operations happen less frequently with higher emission rates per event, and the time of day of the operation is constrained to working hours. Liquid unloadings with manual plunger lifts were simulated as a sensitivity scenario.

Table S3-5. Number of wells assigned liquid unloadings with and without plunger lifts in the basin and two selected counties.

	Number of wells with liquid unloadings with plunger lifts	**Number of wells with liquid unloadings without plunger lifts**
Basin	6685	11214
Bradford, PA	10	17
Wetzel, WV	34	62

S3.13. Gathering and boosting

Gathering and boosting site emissions, including emissions from all fugitive and combustion sources, were simulated at the level of a grid cell, assuming one station per grid cell. Emission rates were estimated using a throughput-normalized emission factor developed based on field measurements, as described by equation (1) [32]:

$$f = 0.0079X^{-0.53} \ (R^2 = 0.45) \quad (1)$$

Where *f* represents the unit-less throughput-normalized emission factor, and X represents the gas throughput in MMSCFD per gathering and boosting station. Whole gas emission rates were calculated by multiplying the throughput-normalized emission factor by gas throughput per station.

Methane, ethane, and VOCs emissions were calculated based on whole gas emission rates and throughput gas compositions at the level of grid cells. Based on field measurements, 38% methane emissions from gathering and boosting stations are due to methane slip [41]. NOx emissions were calculated based on methane slip emissions and engine-specific NOx-to-methane emission factors ratios from AP-42 [30]. For stationary internal combustion sources, NOx-to-methane ratios from 4-stroke lean-burn (4SLB) engines and 4-stroke rich-burn (4SRB) engines are 0.68 and 9.61, respectively. The base case simulation assumed all engines from gathering and boosting sites were 4SLB engines. 4SRB engines were later simulated as sensitivity analyses.

S3.14. Processing plants and transmission facilities

Emissions from gas processing plants and transmission facilities were simulated at the site level. Locations of gas processing plants and transmission facilities were originally sourced from the EPA Greenhouse Gas Reporting Program (GHGRP) [19]. Manual relocating and validation was done based on satellite imagery. A total of 24 gas processing plants and 34 transmission facilities were validated in the simulation domain, shown in

Figure 1 in the main text. Total methane emissions per year per site, reported by GHGRP, were evenly distributed across the year, to calculate hourly methane emission rate. Ethane and VOCs emissions were estimated based on methane emissions and throughput gas compositions from the grid cell in which the midstream site is located.

Methane slip accounted for 66% and 16% of total methane emissions from gas processing plants and transmission facilities, respectively, according to the 2022 GHGI [29]. NOx emissions were estimated using the same method applied to the gathering and boosting sites, based on methane emissions and engine-specific emission factors.

S3.15. Flares

Emissions from flares were simulated at the site level. Flares were identified based on Visible Infrared Imaging Radiometer Suite (VIIRS) observations in 2023 [23]. Annual flare emissions, by flare, were estimated based on annual gas flared volumes, reported by the Earth Observation Group, and an assumed flaring efficiency of 98%. Annual total methane, ethane, and VOCs emissions were estimated based on total gas emissions and grid-level gas compositions. NOx emissions were estimated as 0.49 of uncombusted methane emissions by mass, based on AP-42 emission factors for flaring [30].

The total hours of flaring per site was determined based on the detection frequency in 2023, and an hourly emission rate was calculated per emission species per site, by dividing the annual total emissions by total hours of flaring. Total hours of flaring per site were partitioned into multiple flaring events, with each event lasting up to 240 hours. Flaring events were randomly distributed across the year without temporal overlap.

S4. Base case analyses

S4.1. Base case analyses in Bradford County, PA

Table S4-1. Distributions of methane, ethane, VOCs, and NOx emissions rates in Bradford, PA.

Emission rates statistics (kg/hr)	mean	median	75%	90%	max
Methane	2904	2867	3018	3142	4575
Ethane	64	63	66	69	101
VOCs	4	4	6	8	11
Nox	680	672	708	760	839

Table S4-2. Ratios of maximum to annual average hourly predicted emission rates at the county level, and distributions of the ratios among 132 grid cells in Bradford, PA.

Emissions	Bradford, PA	Distribution of ratios among 132 grid cells in Bradford, PA						
		mean	std	min	25%	50%	75%	max
Methane	1.6	4.8	10	1.0	1.1	1.2	4.3	84
Ethane	1.6	4.8	10	1.0	1.1	1.2	4.3	84
VOCs	2.5	5.0	9.1	1.0	1.1	1.2	5.4	84
Nox	1.2	1.4	1.1	1.0	1.0	1.0	1.0	5.7

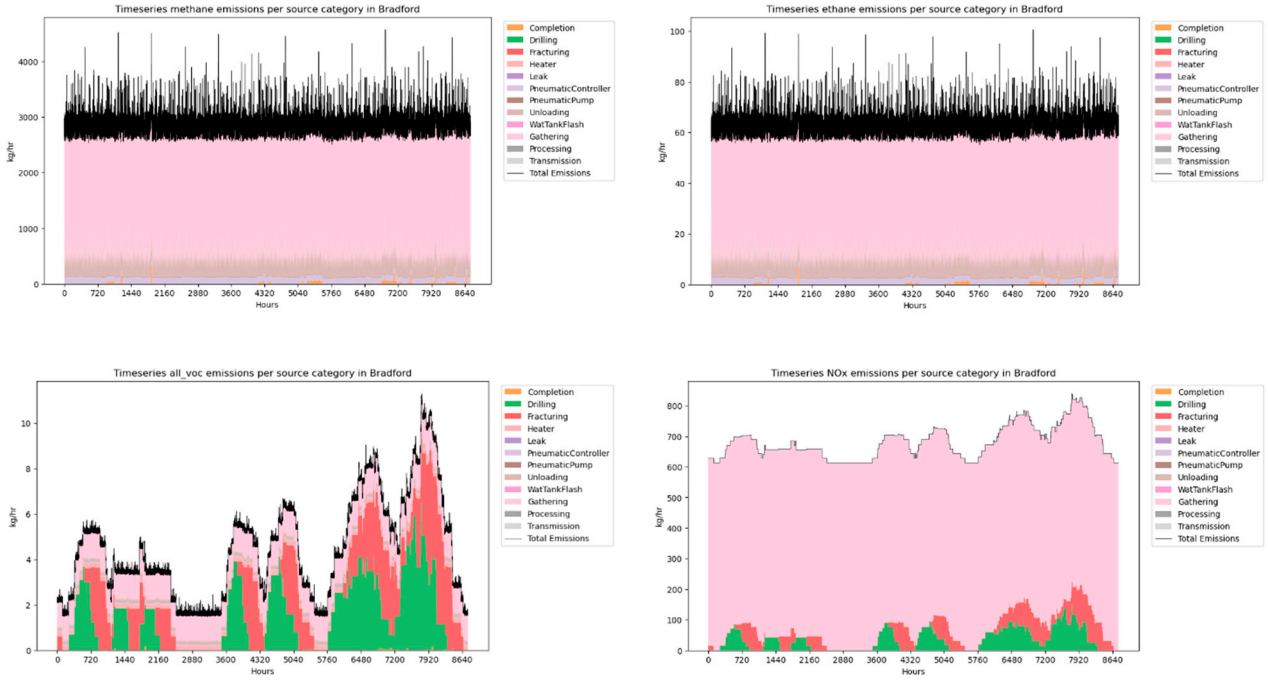

Figure S4-1. Hourly emissions time series for methane, ethane, VOCs, and NOx emissions in Bradford, PA.

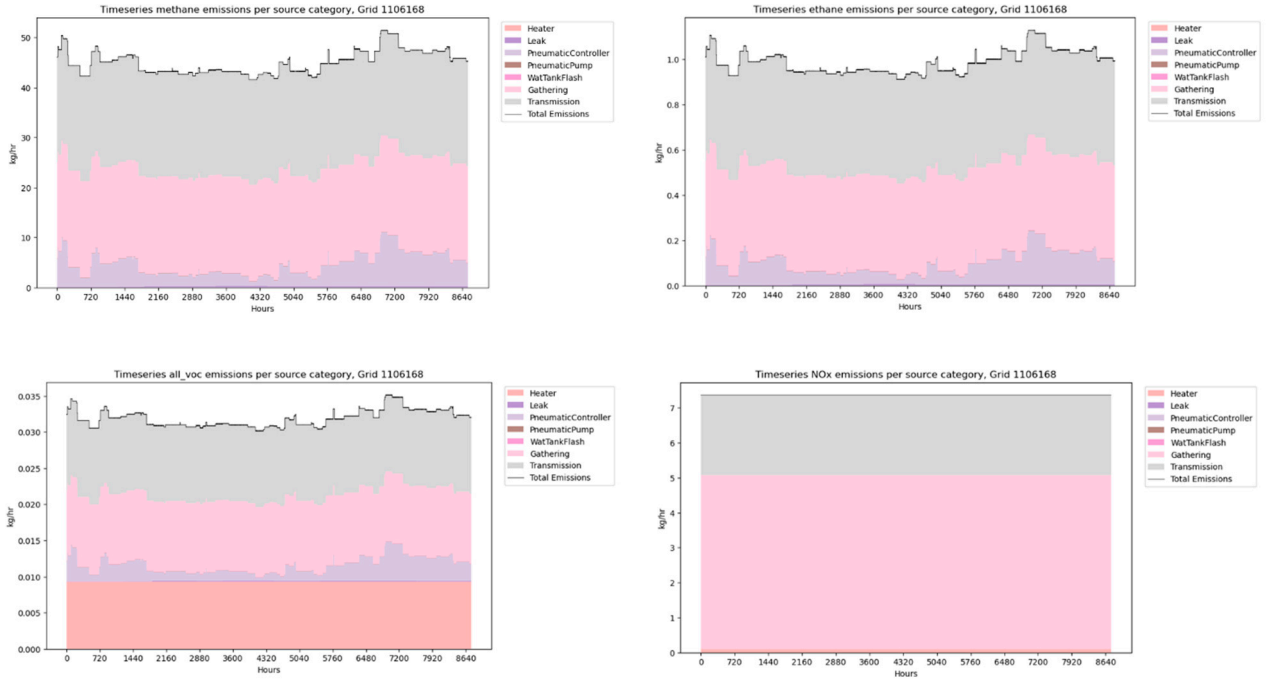

Figure S4-2. Hourly emissions time series for methane, ethane, VOCs, and NOx emissions in Grid Cell 3 in Bradford County, PA.

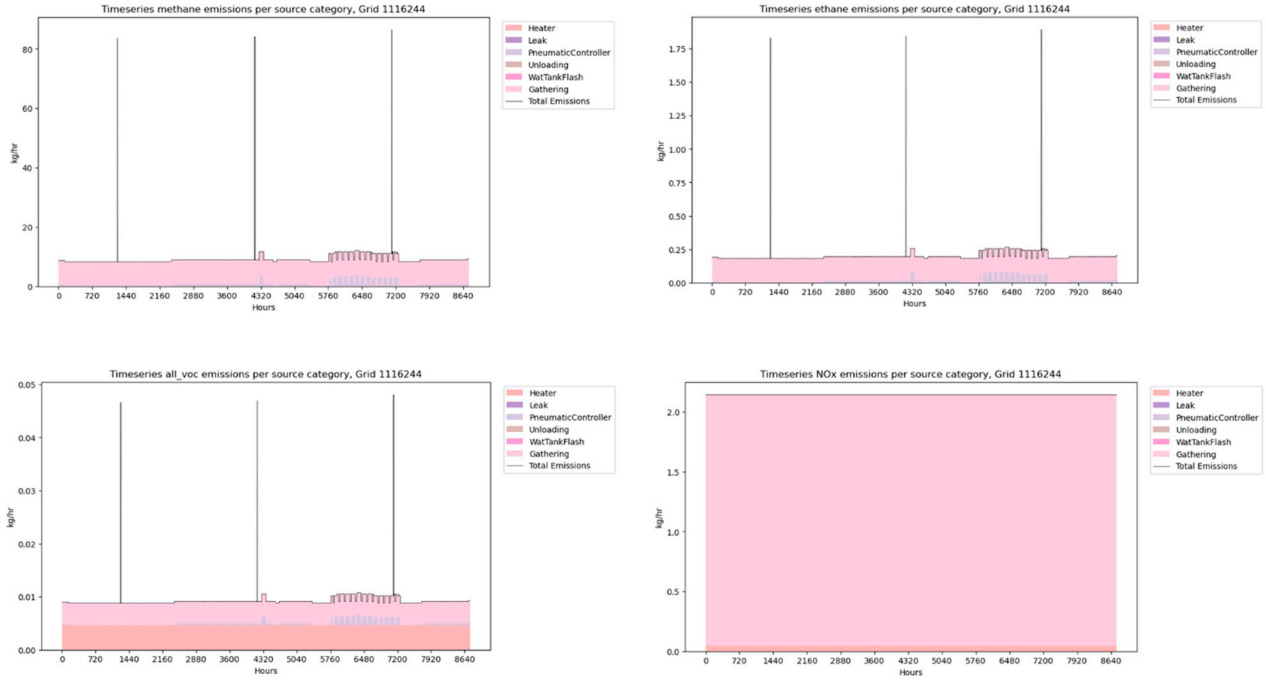

Figure S4-3. Hourly emissions time series for methane, ethane, VOCs, and NOx emissions in Grid Cell 4 in Bradford County, PA.

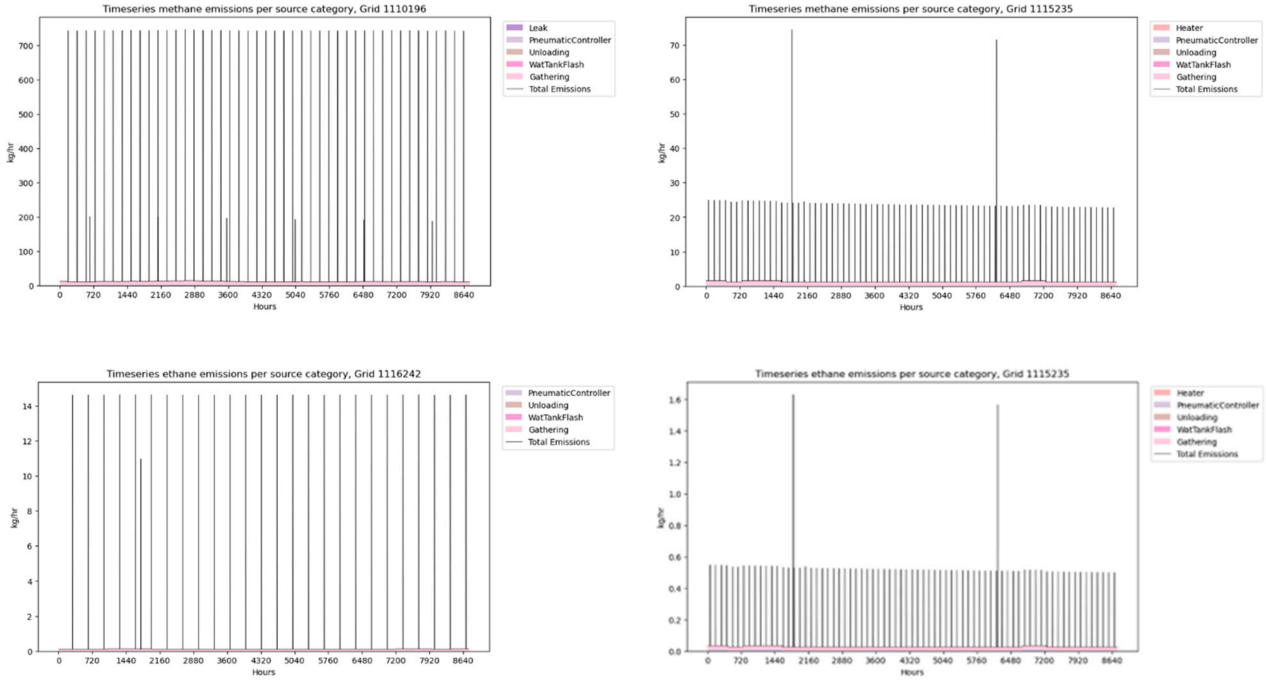

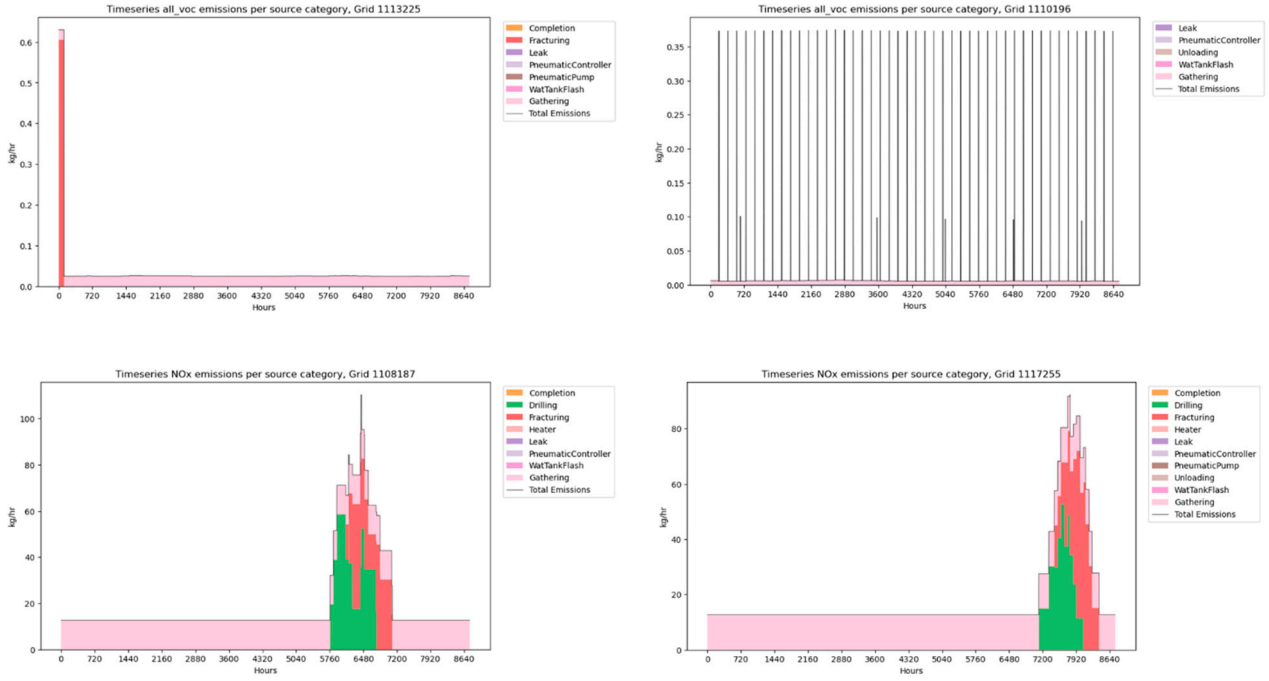

Figure S4-4. Hourly emissions time series for methane, ethane, VOCs, and NOx emissions in grid cells with highest ratios of maximum to annual average emission rates in Bradford, PA. For each emission component, two of the three highest-ranked grid cells were shown as representative examples.

S4.2. Base case analyses in Wetzel County, WV

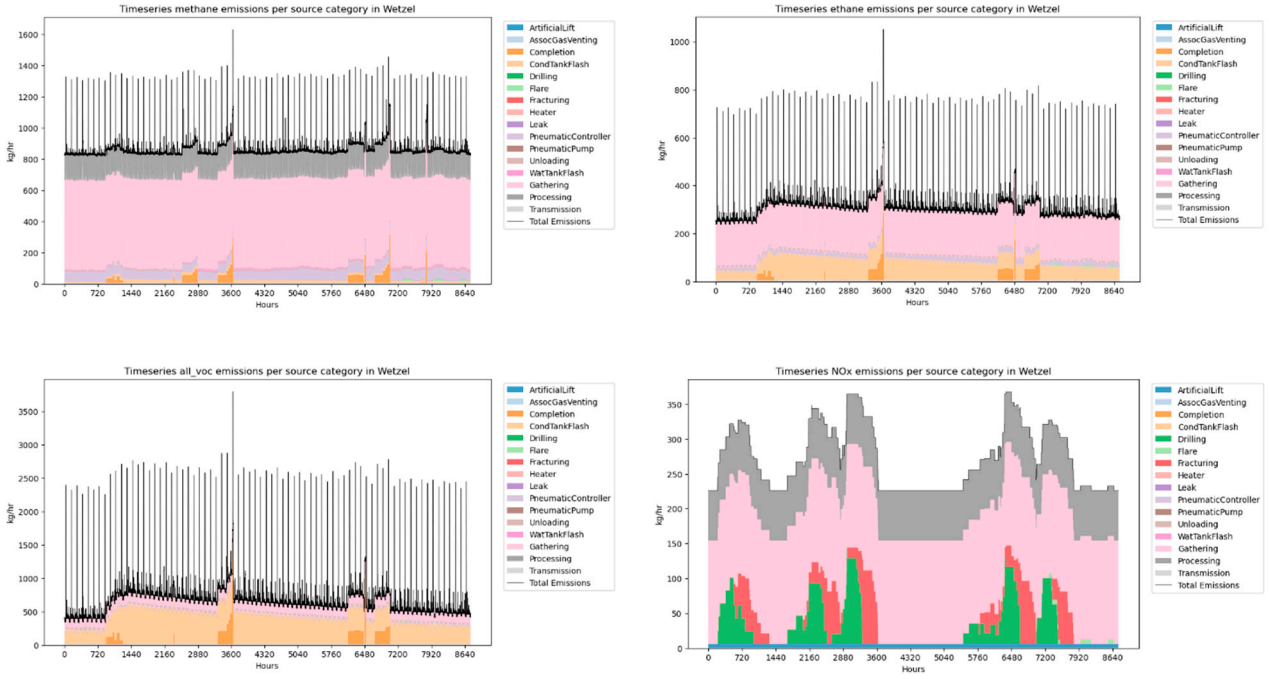

Figure S4-5. Hourly emissions time series for methane, ethane, VOCs, and NOx emissions in Wetzel County, WV.

Figure S4-6. Hourly emissions time series for methane, ethane, VOCs, and NOx emissions in Grid Cell 1 in Wetzel, WV.

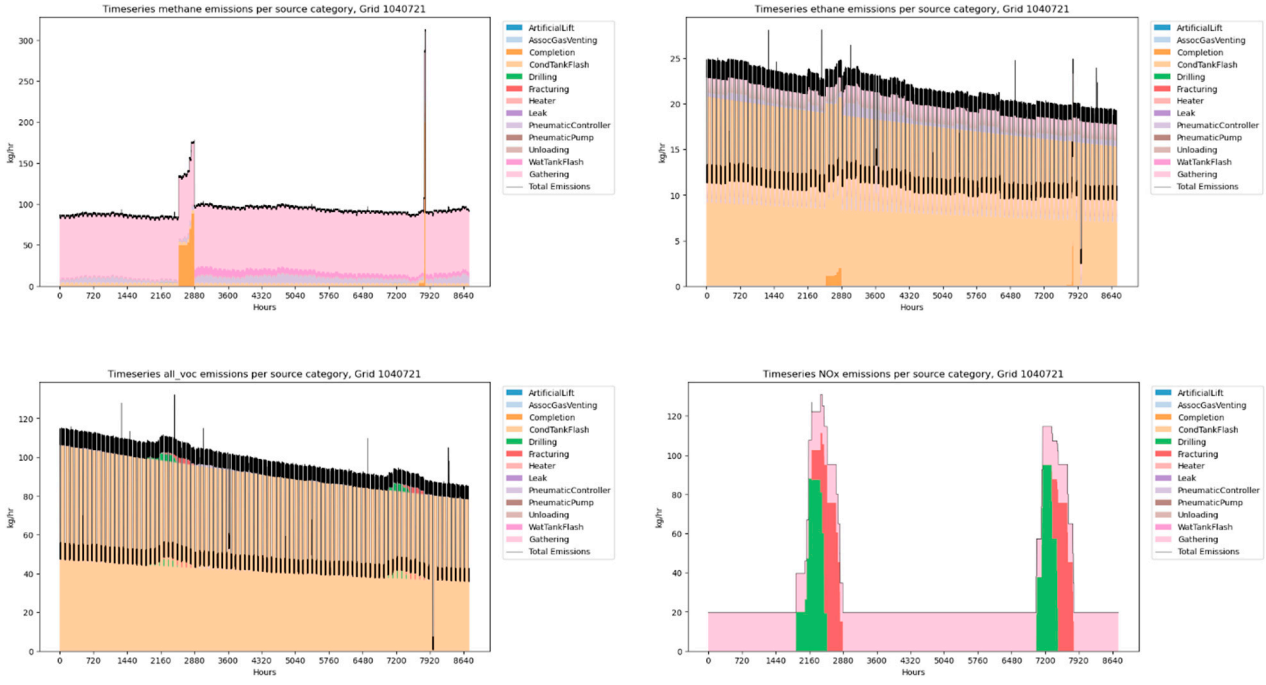

Figure S4-7. Hourly emissions time series for methane, ethane, VOCs, and NOx emissions in Grid Cell 2 in Wetzel, WV (the grid cell presented in the main text).

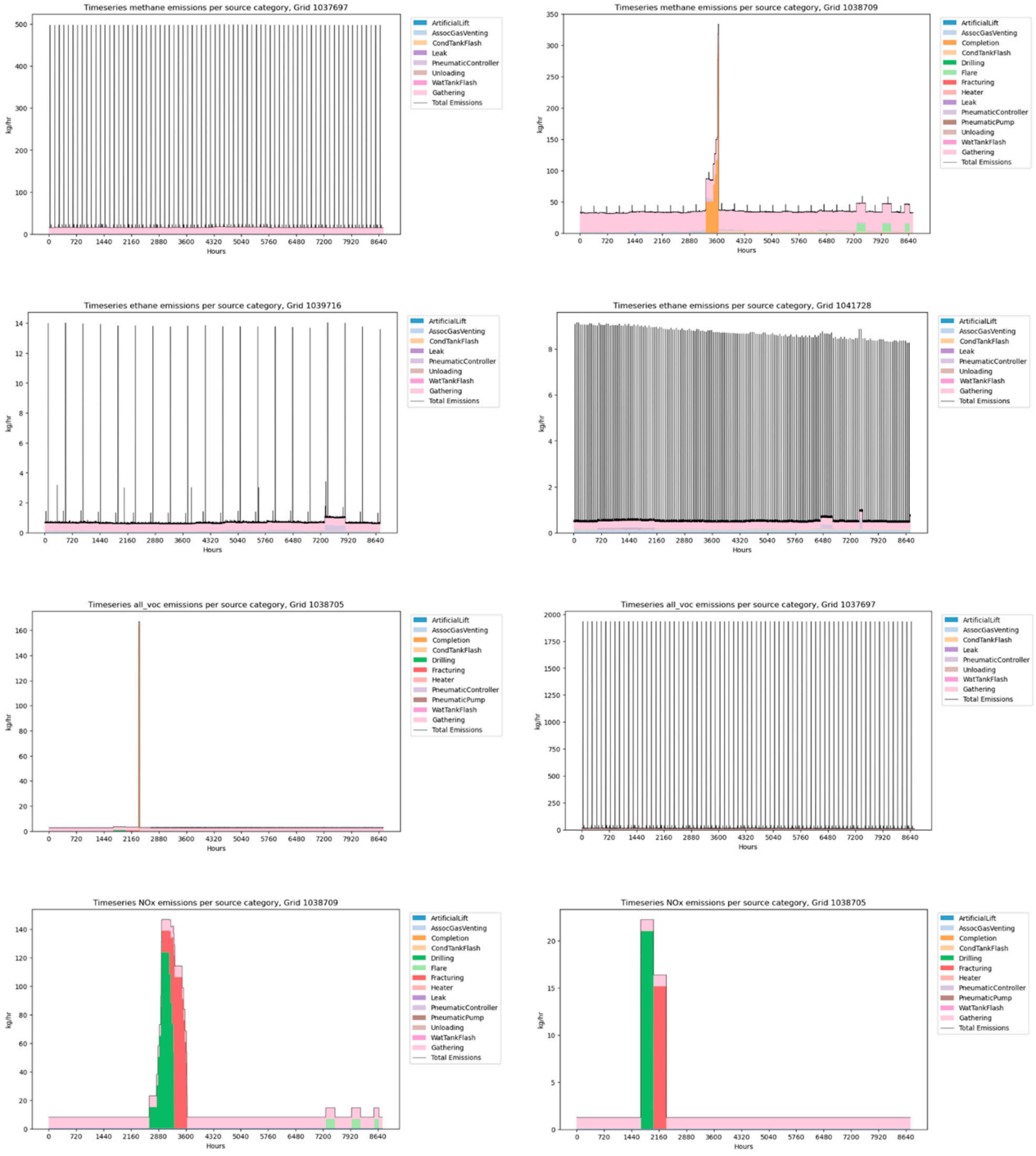

Figure S4-8. Hourly emissions time series for methane, ethane, VOCs, and NOx emissions in grid cells with highest ratios of maximum to annual average emission rates in Wetzel, WV. For each emission component, two of the three highest-ranked grid cells were shown as representative examples.

S4.3. Base case analyses in the basin

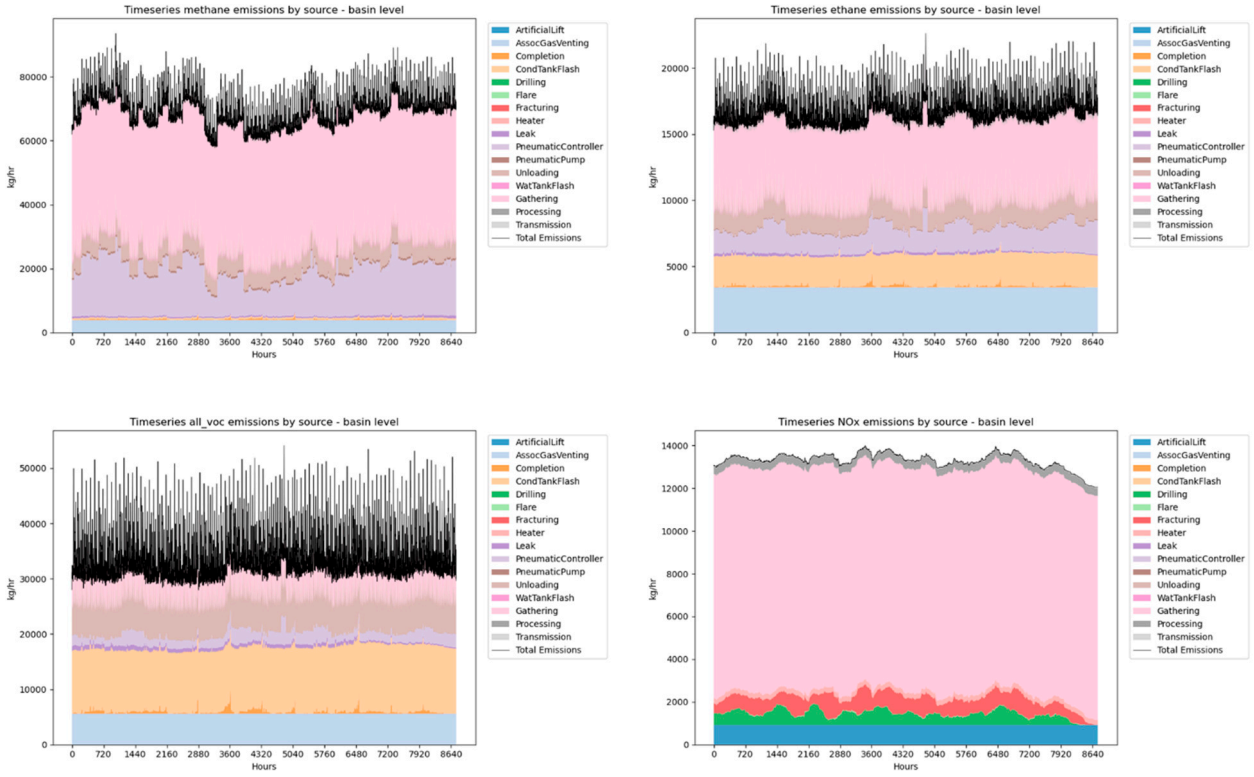

Figure 4-9. Hourly emissions time series for methane, ethane, VOCs, and NOx emissions in the basin.

S5. Sensitivity analyses

S5.1. Emission factors of hydraulic fracturing pumps

Emissions from hydraulic fracturing pumps were calculated using equation (2) [28]:

$$E_i = n \times \frac{EF_i \times HP \times LF \times N_{stages} \times t_{stage}}{907185} \quad (2)$$

where:

E_i is the exhaust emissions for pollutant *i* from a single fracturing event [ton/event]

n is the number of engines used per fracturing event

EF_i is the emissions factor of pollutant *i* [g/hp-hr]

HP is the horsepower of the engine [hp]

LF is the load factor of the engine

N_{stages} is the number of stages per fracturing event [stage/event]

t_{stage} is the duration of the fracturing stage [hr/stage]

907185 is the unit conversion factor [g/ton]

Two sets of fracturing activity factors from the equation above were available in the EPA Oil and Gas Tool [28], as shown in Table S5-1. The base case scenario presented in the main text applied a more recent set of factors developed for Texas basins [37]. The EPA default factors [36] were applied as a sensitivity scenario. Emission factors per pollutant were consistently applied in the two scenarios, shown in Table S5-2. Final calculated emission per event and hourly emission rates after temporal allocation are reported in Table S3-2.

Table S5-1. Two sets of activity factors for hydraulic fracturing engines, extracted from the EPA Oil and Gas Tool.

Fracturing activity factors	Base case scenario	Sensitivity scenario with EPA defaults
Engine horsepower (hp)	2290	1258
Engine load factor	0.49	0.63
Number of stages per event	16.6	5.75
Duration of stage (hr)	2.28	1.5
Number of engines per event (n)	22.5	3.5

Table S5-2. Emission factors for hydraulic fracturing engines, extracted from the EPA Oil and Gas Tool.

Pollutant	Emission factor (g/hp-hr)
CH4	0.0156
VOC	0.213
Nox	5.32

As shown in Figures 2-4 in the main text, across all simulated spatial scales, hydrocarbon emissions from hydraulic fracturing events were negligible compared to other sources. Basin-level hydrocarbon emissions were not sensitive to variations in hydraulic fracturing emission estimates. In contrast, NOx emissions may be substantially influenced by fracturing activities. Figure S5-1 shows the basin-level NOx time series with hydraulic fracturing emissions calculated using EPA default factors. Emissions from hydraulic fracturing events were significantly decreased compared to the base case.

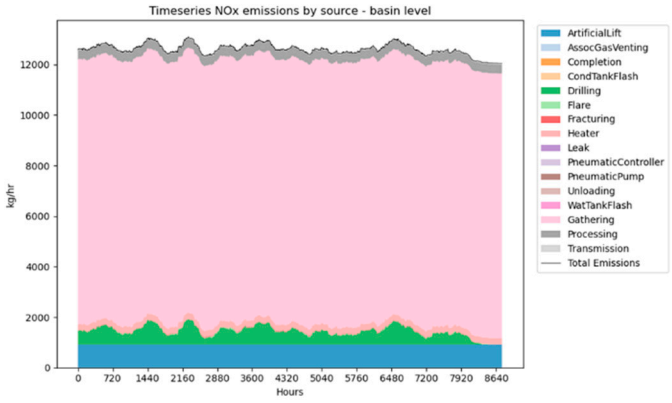

Figure S5-1. Hourly emissions time series for NOx emissions at the basin level, with hydraulic fracturing emissions calculated using EPA default factors.

S5.2. Eliminating pneumatic controllers

Some operators in Marcellus are replacing pneumatic controllers with zero emission devices. Figure S5-2 shows methane time series at the basin level and in Wetzel County, WV, assuming operator X eliminates all its pneumatic controllers. Operator X operates nearly 4000 active wells in the study domain, contributing to 17% gas production in the basin in 2023. Over 300 wells were located in Wetzel, WV, representing approximately 26% of wells and contributing to 45% total gas production in the county.

Eliminating pneumatic controllers from wells operated by Operator X reduced total methane emissions from pneumatic controllers by 50% in the Wetzel County and <2% at the basin level. Impacts on temporal variability of methane emissions at county and basin levels were negligible.

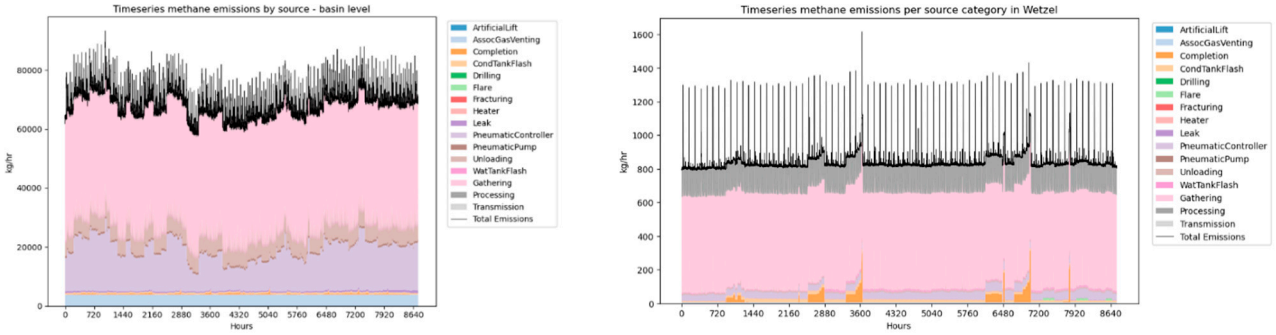

Figure S5-2. Hourly emissions time series for methane at the basin level and in Wetzel, WV, assuming a leading operator replaced all its pneumatic controllers with zero emission devices.

S5.3. Engine types at gas gathering and midstream sites

NOx emissions from gathering, processing, and transmission sites combustion engines were calculated based on estimated methane emissions and NOx-to-methane emission factor ratios from AP-42 [30]. For stationary internal combustion sources, these ratios vary significantly depending on the type of engines. NOx-to-methane ratios from 4-stroke lean-burn (4SLB) engines and 4-stroke rich-burn (4SRB) engines are 0.68 and 9.61, respectively. In the sensitivity scenario shown in Figure S5-3, all engines were assumed to be 4SRB engines. Compared to the base case scenario where all engines were assumed as 4SLB engines, NOx emissions from gathering and midstream sites largely increased, resulting in more consistent NOx emission rates at the basin and county levels. Temporal variability driven by preproduction emissions was largely reduced at the county level and became negligible at the basin level.

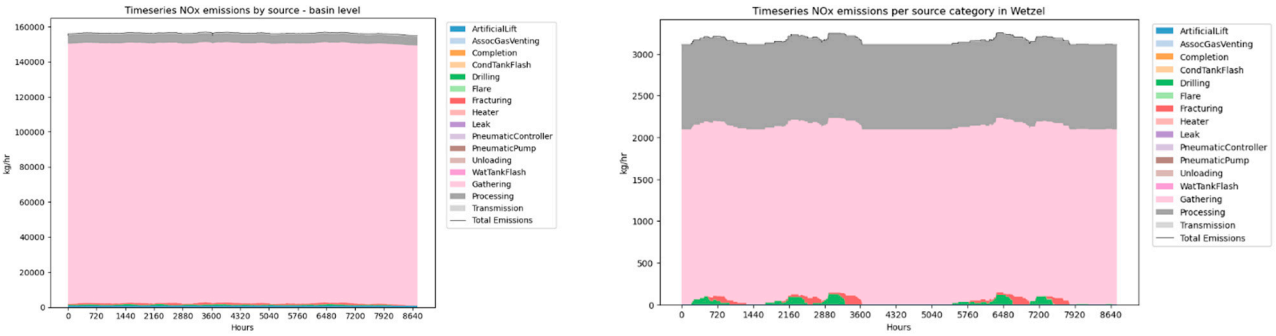

Figure S5-3. Hourly emissions time series for NOx at the basin level and in Wetzel, WV, assuming all compressor engines at gas gathering, processing, and transmission sites were four-stroke rich-burn (4SRB) engines.

S5.4. Liquid unloadings: automated vs manual operations

In Bradford, PA, 10 wells were assigned liquid unloadings with plunger lifts and 17 wells were assigned manual unloadings without plunger lifts. In the base case analyses, all unloadings with plunger lifts were assumed to be automated. Figure S5-4 compares the methane time series with unloadings with automated plunger lifts versus with

unloadings with manual plunger lifts. Compared to the automated plunger lifts, manual plunger lifts happened less frequently with a strong diurnal pattern.

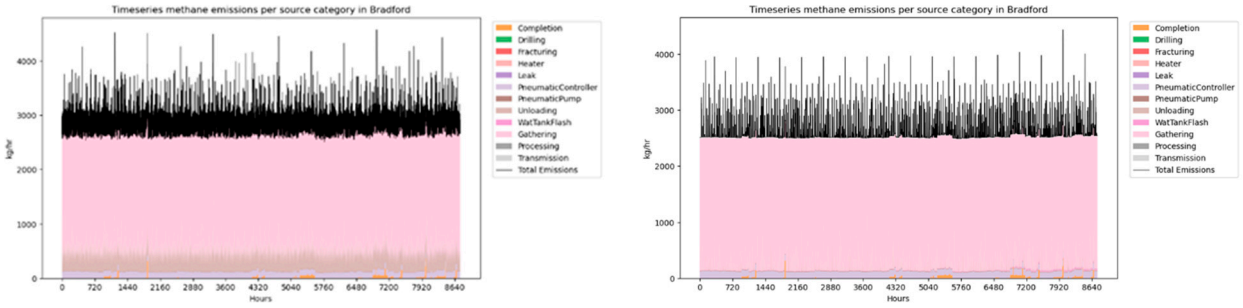

Figure S5-4. Hourly emissions time series for methane in Bradford, PA, with liquid unloadings with plunger lifts assumed as automated (left) and manual (right) operations.

S5.5. Pre-simulation aggregation at the county level

For sources such as pneumatic controllers and pneumatic pumps, pre-simulation aggregation at the county level may introduce bias in county-level emission estimates, as equipment of the same well type within a county are assigned a single emission factor. As shown in Figures S5-5 and S5-6, temporal variability in hydrocarbon emissions due to pneumatic controllers were overrepresented in both counties with pre-simulation aggregation, compared to simulations done at a finer spatial scale prior to county-level aggregation, as shown in the main text.

At smaller spatial scales, such as counties or multi-kilometer grid cell, emission simulations should be performed at the finest spatial resolution possible (e.g., at the well level) to be able to accurately capture the temporal and spatial distribution of emissions. However, there is a tradeoff between estimation accuracy and computational feasibility. Simulating emissions from all individual equipment from well sites is computationally intensive and impractical for basin-wide analyses, such as in the Marcellus, which includes over 200,000 wells. In such cases, pre-simulation aggregation of activity data could be a practical alternative. For example, in the Marcellus study domain in this work, with 173 counties across the basin, the aggregated results at the basin level remain representative, despite potential county-level biases.

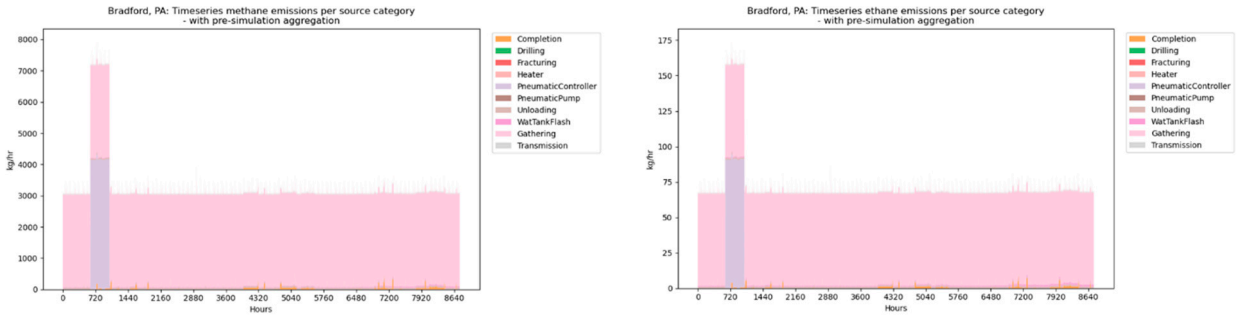

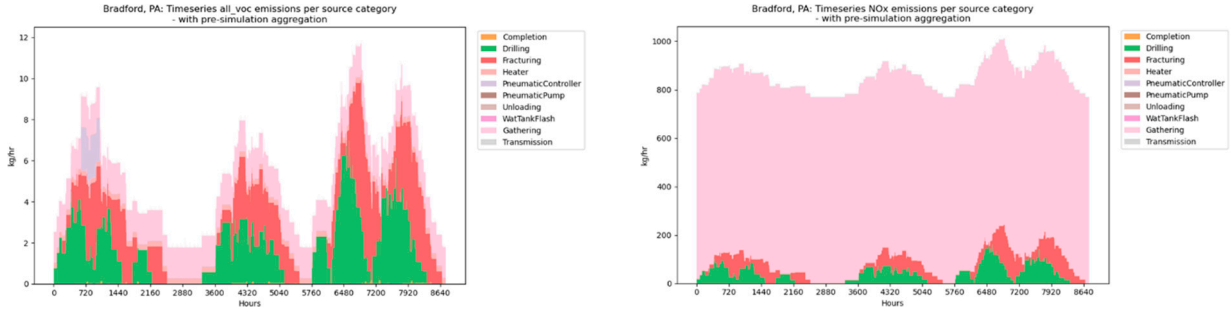

Figure S5-5. Hourly emissions time series for methane, ethane, VOCs, and NOx emissions in Bradford, PA, with pre-simulation aggregation.

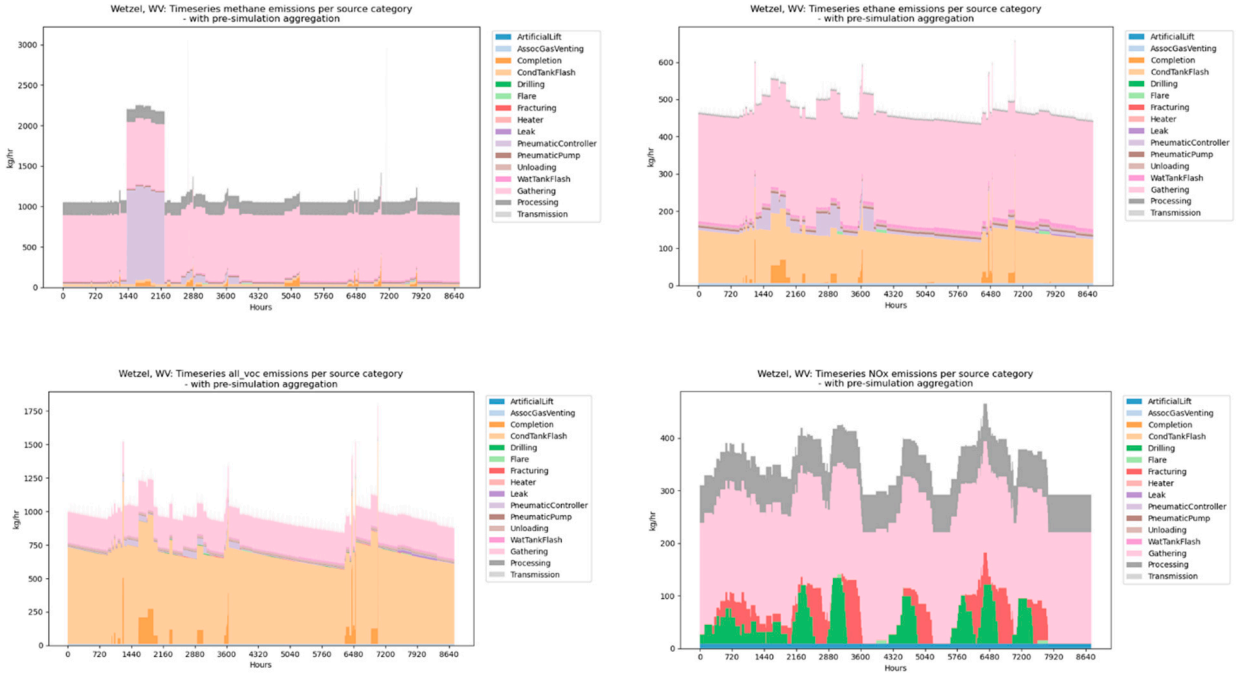

Figure S5-6. Hourly emissions time series for methane, ethane, VOCs, and NOx emissions in Wetzel, WV with pre-simulation aggregation.